

Materials and Methods

MATERIALS AND METHODS

Flowers of Catharanthus roseus (L.) G. Don (Apocynaceae) and Withania somnifera Dunal (Solanaceae) were collected from the plants growing in the Maharaja Sayajirao University campus and were categorised into the following different developmental stages:

1. Stage I - early bud,
2. Stage II - late bud,
3. Stage III - early anthesis,
4. Stage IV - anthesis and
5. Stage V - late anthesis

(Based on the bud size and pistil length).

I. Light microscopy

Pistils at different developmental stages of both the taxa were fixed in FAA (Formalin-Acetic-Alcohol) and processed for microtomy by conventional methods (Berylina and Miksche, 1976). Paraffin sections of 8-10 μ m thickness were taken on a rotary microtome. The slides were de-paraffinised in xylene/tertiary Butyl Alcohol (TBA) series and stained with 0.5% Toluidine blue O in 0.1 M citrate buffer (pH 4.4) or tannic acid/ferric chloride (Jensen, 1962; Feder and O'Brien,

1968). The stained slides were made permanent and were viewed and photographed with a Leitz-Dialux22 microscope using Ilford Black and White film.

II. General histochemistry and cytochemistry

General histochemistry

Proteins: Fresh stigmas/styles were stained in CBB (Coomassie Brilliant Blue) for 5-10 min, and differentiated in 7% acetic acid for 2-5 min. and mounted in glycerine (Heslop-Harrison, et.al., 1973). Sections were also stained with fluorescent dye, 8-Anilino 1-Naphthalene sulphonic acid (Ca^+ salt) (8 ANS-0.001% in 0.1 M Tris pH 7.4) for 5 min. The sections were washed well and mounted in glycerine and observed under fluorescence microscope using UV excitation filter (Stead et.al., 1979).

Lipids: Sudan IV (0.5% in ethyl alcohol), (Jensen, 1962) was used to stain stigma surface lipids. The tissues were differentiated in 50% ethyl alcohol before and after staining and mounted in glycerine. Cutin was localized using the fluorescent dye, Auromine O (0.1% in 0.1 M Tris pH 7.2 (Heslop-Harrison, 1977) after washing the sections in chloroform/methanol in the ratio 1:1 for 5 min. The slides were observed in blue excitation filter with a fluorescence microscope.

Polysaccharides: Iodine-potassium iodide (I_2KI) solution (Jensen, 1962) was used to localize starch in the tissue sections. The tissues were immersed in the solution for 10-40 min, washed and mounted in glycerine. Insoluble polysaccharides were localized using periodic acid - Schiff reaction (PAS) (Hotchkiss, 1948). The paraffin sections as well as fresh stigmas were first oxidised with 1% periodic acid for 10-20 min. to release aldehydes and stained with Schiff's reagent (leucofuschin) for 15-20 min., in the dark. The sections were washed in 2% sodium-metabisulphite and mounted in glycerine.

Enzyme cytochemistry

For enzyme reaction, fresh stigmas were excised, split and immersed in the incubation medium as specified. Omission of the substrate from the incubation medium was used as the control for all enzyme reactions.

Succinate dehydrogenase (SDH, Lillie, 1965)

SDH reaction was carried out using sodium succinate as the substrate in a coupling reaction with Nitroblue tetrazolium (NBT) at pH 7.6. Fresh stigmas were kept in the incubation medium for 15-40 min. at 37°C. Sections were washed well and mounted in glycerine.

Peroxidase (Graham and Karnovsky, 1966)

Enzyme reaction was carried out using an oxidation reaction involving 3-3'Diamino-benzidine tetrahydrochloride (DAB) as the substrate with hydrogen peroxide as a catalyst at pH 7.2. The tissues were placed in the incubation medium for 5 min, washed well in distilled water and mounted in glycerine.

Acid phosphatase (Bancroft, 1975)

The reaction was carried out using sodium β -glycero-phosphate as the substrate involving lead nitrate in a lead precipitation method. Sections were placed in the incubation medium (pH 5) for 30-60 min. at 37°C, washed well in distilled water and immersed in 1% fresh ammonium sulphide solution for 2 min. The sections were washed again in distilled water, and mounted in glycerine.

Adenosine triphosphatase (ATPase-Bancroft, 1975)

The reaction procedure involved a lead precipitation technique using lead nitrate with ATP as the substrate. The sections were immersed in the incubation medium (pH 7.4) for 15-60 min. at 37°C, washed in distilled water, briefly immersed in 1% fresh ammonium sulphide and mounted in glycerine.

Non specific esterase (Brancroft, 1975)

The enzyme reaction was carried out using 1-naphthyl acetate as the substrate in a coupling reaction with hexazotised para-rosanilin HCl. Sections were immersed in the incubation medium (pH 7.2) for 15-60 min. at 37°C, washed in distilled water and mounted in glycerine.

III. In vitro pollen-germination

Flowers from the two plants were collected around 8 a.m. Pollen grains from freshly dehisced anthers were dusted in semi-solid agar blocks taken on a slide. The nutrient medium contained the following nutrients (Brewbaker and Kwack, 1963) and were later modified for getting maximum pollen germination and tube growth.

Medium composition

Boric acid	- 10 mg	Magnesium sulphate	- 40 mg
Calcium nitrate	- 60 mg	Potassium nitrate	- 20 mg

Suitable concentrations of sucrose and 1% agar were added and small blocks were cut from the solidified medium. These agar blocks were placed on a moist filter paper in a petri-dish to maintain humidity.

Pollen germination and tube growth were noted at regular time intervals. The pollen tube length was measured using

ocular and stage micrometers. In each case, five separate experiments were run simultaneously. All the pollen germination studies in vitro were carried out at $30 \pm 1^\circ\text{C}$ at 90% RH and under laboratory light conditions.

IV Effect of self and cross pistil extracts on in vitro pollen germination

For studying the effect of self and cross pistil extracts on pollen germination, styles (along with stigmas) from unpollinated flowers were homogenised in an ice cold mortar in 0.015 M phosphate buffer at pH 5.9 (10 pistils/ml in the case of Catharanthus and 20 pistils/ml in the case of Withania). The extracts were centrifuged at 10,000 g at 5°C and the supernatant of self and cross pistil extracts were incorporated in the pollen culture medium separately. Pollen germination and tube growth were recorded after 2 h.

V In vivo pollen germination

In vivo pollen germination was carried out by hand pollinating the excised pistils taken from the inflorescence covered with polythene bags and brought to the laboratory around 8'0 clock in the morning. Pistils from previously bagged flowers/inflorescence were excised and implanted in solidified agar in petridishes. Stigmas were pollinated using pollen grains taken from freshly dehisced anthers with the help of an eyelash brush under a stereo microscope. Cross pollen and self pollen

were used in separate experiments. The hand pollinated pistils were fixed overnight in acetic alcohol in the ratio 1:3 at definite time intervals, cleared in 8 N NaOH for 8 h and were stained in 0.005 % decolourised aniline blue in phosphate buffer pH 8.4 (Linskens and Esser, 1957). The pistils were split open longitudinally with a needle before mounting. The stained tissues were observed with a Leitz Dialux-22 microscope with epifluorescence attachment under UV excitation and photographed using Ilford 400 ASA black and white and Konica 100 ASA day light colour film.

VI Effect of sulphur dioxide on *in vitro* pollen germination

Pollen grains from freshly dehisced anthers were dusted on nutrient agar blocks kept on slides on top of a moist filter paper. The petri dishes were then kept in the fumigation chamber. Sulphur dioxide in the chamber was created by the reaction procedure using sulphuric acid and sodium sulphite (Rao and Pal, 1975).

For studying the *in vivo* effect of SO₂, the whole inflorescence were subjected to sulphur dioxide exposure of varying concentrations separately (0.5, 1, 1.5 ppm) for 1 h prior to pollination. Pollination was carried out using SO₂ treated pistil versus normal pollen and vice versa for all the concentrations. Pollination involving normal pistil and normal pollen was considered as the control. The pollinated pistils

were fixed after 2 h in 1:3 acetic acid alcohol and processed for fluorescence microscopic observation.

VII Effect of spermidine^(spd) and MGBG on *in vitro* pollen germination

Pollen grains from freshly dehisced anthers were germinated in the nutrient medium (Brewbaker and Kwack, 1963), supplemented with various concentrations of spermidine or MGBG (Methyl glyoxal-bis(Guanylhydrazone)) or actinomycin-D alone or in combination. Pollen tube growth was measured using ocular and stage micrometers.

VIII Pollen viability

Pollen grains from freshly dehisced anthers were collected, wrapped in thin transparent paper and kept in plastic vials and made airtight. The plastic vials were kept at -4°C, 4°C, dessicated condition, and at room temperature. Viability tests were carried out on each day using Evan's blue (0.5 % aqueous, Jensen, 1962) and fluorochrome, fluorescein diacetate (FDA), (Heslop-Harrison and Heslop-Harrison, 1977). (2 mg of FDA dissolved in 1 ml of acetone was added to the liquid pollen germination medium drop by drop, till the solution becomes cloudy. The pollen grains were dusted on to the drop of the stain and observed under UV excitation).

IX Estimation of total protein

A known amount of fresh tissue was homogenised in 0.1 M Tris-HCl buffer, pH 7.2, and centrifuged at 6,000 g for 10 min. The protein content in the supernatant, after appropriate dilution, was determined according to the method described by Bradford (1976).

Preparation of Bradford's reagent

10 mg of Coomassie Brilliant Blue (CBB) G250 was dissolved in 5.6 ml of absolute alcohol. 10 ml of orthophosphoric acid was added, and the solution was made up to 100 ml.

X Preparation for Electron microscopy

For transmission electron microscopy, different stages of stigma/style and anthers were fixed in 6% glutaraldehyde in 0.2 M cacodylate buffer, pH 7.0 for 2 h at 4°C. After thorough washing in buffer, the tissues were post fixed in 2% osmium tetroxide (OsO_4) in the same buffer for 10 h at 4°C, washed in the buffer and dehydrated through graded series of acetone. The tissues were finally embedded in a low viscosity epoxy resin (Spurr, 1969). Thick and thin sections were cut with glass and diamond knives on Jeol Jem Ultramicrotome. Silver-grey sections picked on formvar coated copper grids were stained with uranyl acetate followed by lead citrate and examined with Jeol 100x

Transmission Electron Microscope. The photographs were taken on ^{OR WO} NP 22 plate film.
K

For scanning electron microscopy, the tissues were fixed in 6 % glutaraldehyde in cacodylate buffer pH 7.0 for 2 h and dehydrated in a graded series of acetone. The tissues were mounted on aluminium stubs, coated with gold/palladium and viewed with a Cambridge Stereoscan S₄¹⁰ Scanning Electron Microscope.

yields two important alkaloids, viz. vincristine and vinblastine which are used in the treatment of cancer. The juice of the leaves is applied to wasp sting. It yields also an alkaloid which is heart poison.

2. PISTIL

2.1 STIGMA

The mature stigma in C. roseus is a massive dumb-bell shaped structure and is of wet type, with a viscous exudate bathing the whole stigma surface (Fig.1.1A). Stigmatic head consists of highly vacuolated cells with peripheral cytoplasm. The epidermal cells are elongated to form papillae cells (Fig.1.1B). The papillae cells are unicellular and are of two types. The papillae cells at the tip of the stigmatic head and bottom are more elongated than those on the lateral surface (Fig.1.1C). The long papillae cells are highly vacuolated and are arranged in a radiating pattern. Each papillae cell has a cuticular lining (1.1D), dense cytoplasm with small vacuoles and a thick cell wall. Some of the papillae cells are densely stained (Fig.1.1E). The stigma consist of three distinct regions. The upper region of the stigma has compactly arranged highly vacuolated cells. The lower portion of the stigma consists of a central column of compactly arranged cells and loosely arranged cells at the periphery (Fig.1.1F). The intercellular spaces on the periphery contain secretory

fluid through which the pollen tube grows (Fig.1.1F). The secretory fluid is present abundantly on the sides of the stigma head and are only sparsely present on the upper surface (Fig.1.1A). The vascular bundles extend only upto the lower region of the stigmatic head. The basal periphery of the stigma extends down forming a hollow flap like structure encircling the upper stylar region. It consist of 8-10 layers of highly vacuolated and elongated cells (Fig.1.2A). The loosely arranged transmitting tissue extends upto the junction of the style and the stigma flap and is continuous with the transmitting tissue of the style (Fig.1.2B, 1.2C).

2.1.1 Development of the stigma

At stage I, the stigma is represented by a homogenous mass of cells. The epidermal cells show slight protuberances which are loosely arranged radially, and are highly vacuolated (Fig.1.2D). No exudate is discernible at this stage. The papillae cells elongate subsequently in stages II to IV (Fig. 1.2E), those on the upper side of the stigma and the lower region show maximum elongation. This development leads to the formation of two distinct type of papillae cells. The papillae cells become glandular and starts secreting by stage II onwards (Fig. 1.2E). By stage V the smaller papillae cells along the sides show degeneration (Fig. 1.2F).

2.1.2. Ultrastructure of the stigmatic head

C. roseus stigma shows a sticky exudate in the receptive stage, bathing the entire surface of the dumb-bell shaped stigma head. The stigma has unicellular long papillae cells at the tip and the base. Those along the sides are smaller, have uniform length and are compactly arranged. Both the types of papillae cells are glandular and secrete the stigma fluid.

Long Papillae: The cytoplasm of this type of papillae cells are less dense and is highly vacuolated (Fig. 1.3 A,B). Their cell wall has highly dispersed microfibrils and contain osmiophilic materials embedded within the microfibrils (Fig. 1.3 C,D). Plasmodesmatal connections are absent in this cell wall while they are abundant on the common wall between the papillae cell and the basal cells (Figs. 1.3A, 1.4B, arrows). The cytoplasm contains abundant smooth and rough ER, plastids, mitochondria and dictyosomes (Fig. 1.3B, C).

Plastids are dense with little internal membrane system, but contain small dark osmiophilic droplets (Fig. 1.5B, C, arrows). Some of them also contain pro-lamellar bodies and few poorly stacked thylakoids (Fig. 1.5D). Many of them are closely associated with ER, often completely encircled by it (Figs. 1.4D, 1.5D),

Mitochondria, usually spherical or oval in shape, are numerous in the cytoplasm (Figs. 1.5A,C,D; 1.6A). They have abundant cristae and many of them are closely associated with osmiophilic droplets (Figs. 1.5C; 1.6A,B). Dictyosomes of the golgi complex usually distributed near the wall of the papillae, produce large (Fig. 1.5B), and small vesicles (Figs. 1.3C; 1.6B). Endoplasmic reticulum both smooth and rough are associated with osmiophilic droplets (Figs. 1.5C; 1.6A,B, arrows). Some of the cisternae are also aligned along the wall and associated with the membrane (Figs. 1.4D; 1.6A,C). Vacuoles are small and numerous during the secretory stage of the papillae. They contain many multilamellate structures and vesicles probably depicting membrane turnover (Figs. 1.3A; 1.4B). The plasma membrane along the wall of the papillae cells are undulated and accommodate numerous vesicles. Some papillae cells also show large vacuoles filled with fibrillar materials. The cell wall has highly dispersed microfibrillar texture and many vesicular structures and osmiophilic material are found amidst the microfibrils and outside the wall (Figs. 1.3D; 1.4B) probably depicting the active release of the secretory materials.

Short Papillae: This type of papillae cells are uniform in size and compactly arranged along the lateral sides of the stigmatic head. Their cytoplasm in the early stage of secretion (II & III) is dense with abundant polysomes, free

ribosomes, dictyosomes, mitochondria, profuse ER and few plastids (Fig. 1.7A-D). However, in the later stage (IV) vacuolation increases in the cytoplasm (Fig. 1.8A,B) which ultimately leads to a highly vesiculate cytoplasm in stage V (Fig. 1.8B). The cell wall shows highly dispersed microfibrils. Small vesiculate structures along with osmiophilic material are abundant amidst the microfibrils (Fig. 1.8B arrows).

The synthesis and secretion stages of the papillae cells are marked by an organelle rich cytoplasm. The cytoplasm is dense and has few vacuoles, the vacuoles invariably contain fibrillar material (Fig. 1.9A,B). Large osmiophilic droplets accumulate in the cytoplasm of the cells from stages III & IV prior to their elimination from the protoplast (Fig. 1.9A). The most prominent organelles in the cytoplasm at this stage are smooth and rough ER, mitochondria, dictyosomes and plastids.

ER is usually smooth, its cisternae runs along the radial and tangential walls (Fig. 1.9B-C), and profusely distributed in the cytoplasm (Fig. 1.10B). Osmiophilic material, as droplets, is usually associated with the ER cisternae (Fig. 1.9B-C), ER also forms close association with the plasmalemma of the radial and tangential walls (Fig. 1.9B,C) and sometimes, the cisternae fuse with the plasmalemma invaginations (Figs. 1.9C; 1.10D). Osmiophilic

material is also seen within the wall below the ER plasmalemma association possibly depicting its role in elimination of the osmiophilic material.

The other prominent organelle present in the cytoplasm of short papillae cells is the hypertrophied dictyosomes (Figs. 1.9B,C,D; 1.10A; 1.11B,D; 1.12A). The dictyosomes produce two different types of vesicles depending on the stage of secretion in the papillae cells. Those in stages II & III produce smaller dense vesicles (Figs. 1.9B,C; 1.10A), while in stages IV & V they produce large translucent vesicles (Fig. 1.11B). The former vesicles are dispersed in the cytoplasm and sometimes form multivesicular bodies (Fig. 1.9C), and probably are secreting the polysaccharide component of the secretion product. The larger vesicles do not contain any visible apparent secretion product in them (Fig. 1.11B) but, the accumulation of large number of vesicles in stage V and their subsequent fusion lead to the highly vacuolated cytoplasm (Fig. 1.8A,B,C), which is indicative of the eventual senescence and death of papillae cells.

Mitochondria are comparatively smaller and they have sparse cristae (Figs. 1.10A,B; 1.11B,D). They may be freely distributed in the cytoplasm (Fig. 1.10B) or aligned near the wall (Fig. 1.10B). Many of them are associated with osmiophilic droplets (Fig. 1.10A). Plastids are few with poorly developed internal membrane system, and do not contain starch or osmiophilic droplets (Figs. 1.8A; 1.11C; 1.13A).

Cell wall of the papillae cell, shows highly dispersed microfibrillar texture even in the early stages and the plasmalemma is highly undulated (Fig.1.11A arrows). Plasmalemma undulations become more pronounced in stage IV and finely distributed, highly dispersed cell wall material is found within these invaginations depicting wall membrane apparatus similar to transfer cells (Figs.1.10C; 1.12B). The dispersal of cell wall material becomes more evident in this stage, probably due to the active secretion through vesicular structures which get embedded within this (Figs.1.12A; 1.13A-D). Dark osmiophilic material is also seen amidst the microfibrils in the wall (Figs.1.10D; 1.12A;1.13A).

The sub-papillae cells also show a highly electron dense cytoplasm (Fig.1.14A), while those below them have highly vacuolate electron translucent cytoplasm (Fig.1.14B,C). Plastids, mitochondria and dictyosomes are abundant in the sub-papillae cells and osmiophilic materials are seen within the cell wall, indicating their participation in secretion and exchange of material. Mitochondria in the cells below the sub-papillae cells have sparse tubular cristae.

2.2 STYLE

The style is of the solid type consisting of elongated parenchymatous cells, flanking a central column of loosely arranged cells forming the transmitting tissue (Fig.1.15A). Three vascular bundles are distributed around the transmitting

tissue, and pass uninterrupted through the length of the style (Fig.1.15 B). The intercellular space between the transmitting tissue cells show abundant secretory material (Fig.1.15 C).

2.2.1 Ultrastructure of the transmitting tissue

Transmitting tissue, prominently developed below the stigmatic head at stage II are elongated compactly arranged cells with intercellular spaces between them (Fig.1.16A-D). Nucleus in them is usually elongate, fusiform or elliptical and have dispersed chromatin (Fig.1.16A,B,D). In some of the cells, two fusiform nuclei lying side by side are observed (Fig.1.16A). The cytoplasm of the transmitting tissue cells are seen with little vacuolation and abundant organelles. One of the remarkable features at this stage is the profuse dilated smooth ER cisternae in the cytoplasm (Fig.1.16B,C,D,arrows). Mitochondria are numerous with dense matrix and cristae (Fig.1.16 B, C,D). Plastids are of two types, one almost spherical with poorly developed internal membrane system (Fig.1.17A,D) and the others which are long with well developed chloroplasts (Figs.1.17C; 1.18A,B). Some of the chloroplasts are very large filling almost three fourth of the cell lumen in cross sectional view and contain starch and osmiophilic droplets (Fig.1.18A). The cell wall in stage IV separate at the radial walls and dispersed dark materials are seen in the middle lamella region (Fig.1.17C) or contain secretory material (Fig.1.17D). Growing pollen tubes are seen

amidst the intercellular substance even in stage IV (Fig.1.17D, arrow). Section of the style at stage V shows profuse growing pollen tubes in this tissue (Fig.1.18C,D).

2.3 HISTOCHEMISTRY OF THE STIGMA

Histochemical observations are done on both fresh and F.A.A. fixed stigma/style. Observations were made on stigma papillae and adjacent tissues and the exudate. Terminology to describe the varying intensities of localization is used for an overall picture of staining, eventhough, a group of cells in a tissue may show varying degrees of localization reaction.

The exudate is insoluble in water and completely soluble in chloroform/methanol (1:1). The exudate stains intensely for lipids when stained with Auromine O and sudan IV in all stages (Fig.1.19^AC). The exudate also stains intensely for insoluble polysaccharides following PAS reaction (Fig.1.19B).

The intact cuticle lining over the papillae cell is localized by Auromine O staining (Fig.1.19B). Protein deposition is meagre in the papillae cell cytoplasm as well as on the papillae surface during stages I & II whereas, in the later stages, the papillae cell walls show intense deposition of protein (Fig. 1.19D). The papillae cell cytoplasm shows meagre to moderate staining for proteins

in the later stage (Fig. 1.19E). Biochemical estimation of stigma/style extracts also show a low protein in the early stages, while the later stages show high protein content (Fig. I).

2.4 ENZYME CYTOCHEMISTRY OF THE STIGMA

Peroxidase

Peroxidase activity is granular and moderate in the cytoplasm of papillae cell at stages I & II (Fig. 1.20A) Whereas, it is meagre in the stages III & IV. The cells below the stigma papillae also show moderate peroxidase activity in the early stages and is undetectable in later stages.

Succinate dehydrogenase

SDH activity is meagre to moderate in stages I & II whereas, in the later stages intense activity (Fig. 1.20B) in the cytoplasm towards the tip of the papillae cell is observed.

Adenosine triphosphatase

ATPase activity in the papillae cells is granular and moderate to intense in all stages of stigma development (Fig. 1.20C).

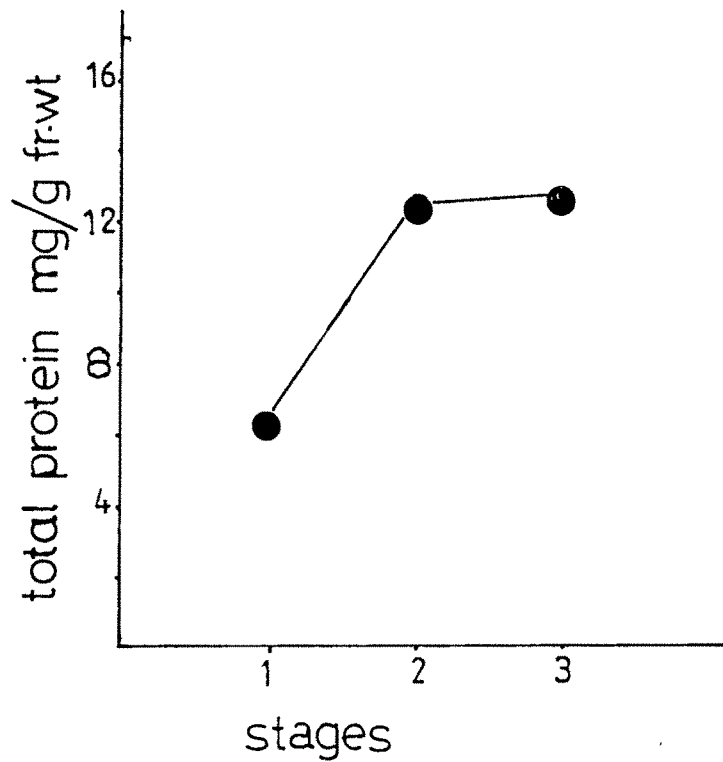


Fig. I. Graph representing total proteins in the stigma/stylar extracts at different stages in C. roseus.

Stage 1 - (Early bud and late bud);

Stage 2 - (Early anthesis)

Stage 3 - (Anthesis and late anthesis).

Non-specific esterase

The papillae cells in stages I & II show meagre to undetectable activity of non-specific esterase. Intense activity was observed in the papillae cells of stages III & IV (Fig. 1.2CE). The exudate shows moderate activity of non-specific esterase in the later stages of stigma development.

Acid phosphatase

The late senescent stages of the stigma show intense activity for acid phosphatase in the papillae cells. The activity is localized both as wall bound as well as in the cytoplasm of the papillae, towards the tip (Figs. 1.2OD; 1.2OF). The early stages show meagre to undetectable activity.

3. MICROSPOROGENESIS AND MEGASPOROGENESIS

3.1 Anther

Mature anther is bithecous and tetrasporangiate. Each microsporangium consists of an outer epidermis, an endothecium, 2 middle layers and 1 or rarely 2 layers of tapetum which is secretory, and a central mass of sporogenous tissue (Fig. 1.21A).

3.1.1 Microsporangium

The young microsporangium consists of homogenous mass of cells surrounded by the epidermis (Fig. 1.21B). It becomes four lobed and a vertical row of hypodermal archer-

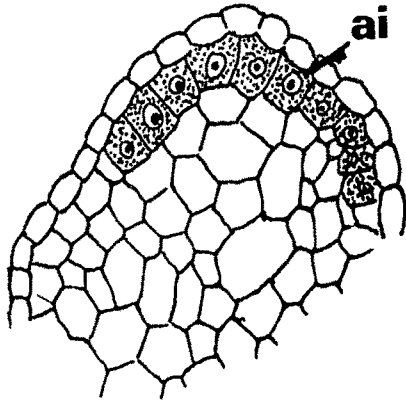
porial cells differentiate in each lobe. They divide periclinally to form the primary parietal cells and primary sporogenous cells (Fig. A_1). The primary parietal cells divide to form the secondary parietal cells. The inner secondary parietal cells give rise to the tapetum whereas the outer secondary parietal cells form a double layered endothecium (Fig. 1.21C) and middle layers (Figs. A_2, A_3).

The inner derivatives of the secondary parietal cells become radially elongated and densely stained with prominent nucleus to form the tapetal cells (Fig. 1.21D). As the sporogenous cells undergo repeated mitotic divisions, the tapetal cells separate and form the middle layers (Fig. 1.21E). They undergo repeated anticlinal and occasional periclinal divisions to form a single layered or irregularly two layered uninucleate tapetum in juxtaposition to the sporogenous cells. In the microspore mother cell stage, the tapetal cells lie along the periphery of the microsporangium and are separated from each other (Fig. A_4). The tapetum is of the secretory type since it persists up to the late stage of microsporogenesis (Fig. 1.21F).

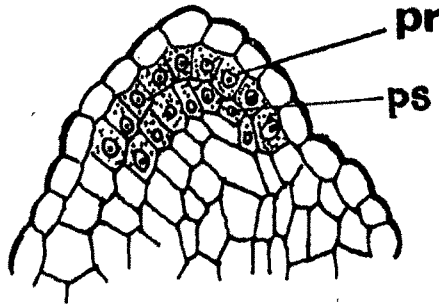
3.2 Microsporogenesis

The primary sporogenous cells divide in all planes repeatedly to form the microspore mother cells (Figs. A_1, A_2, A_3). The first meiotic division is always followed by wall formation thus having successive type of

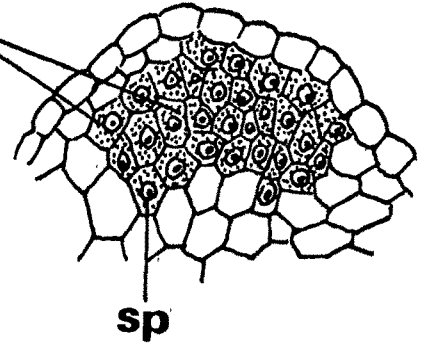
Fig-A



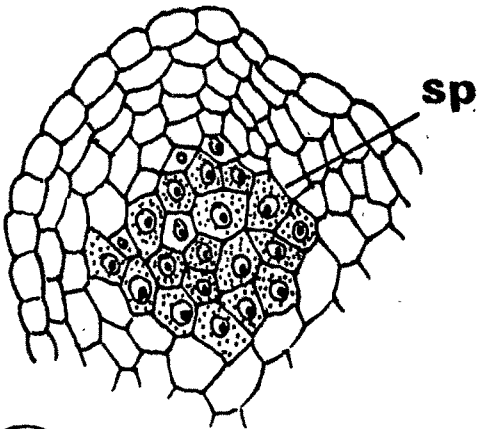
A₁



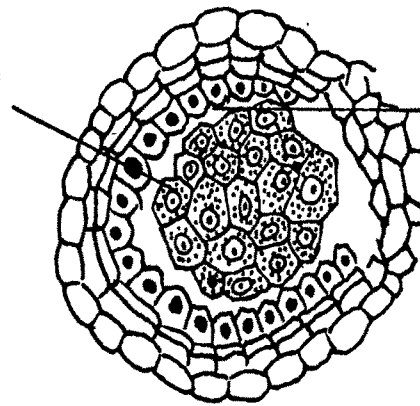
A₂



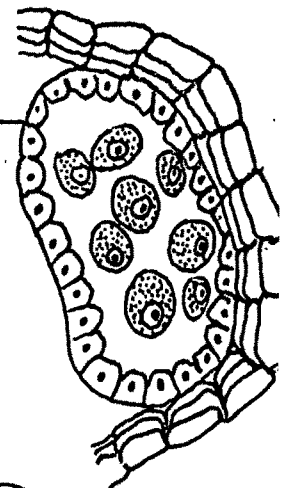
A₃



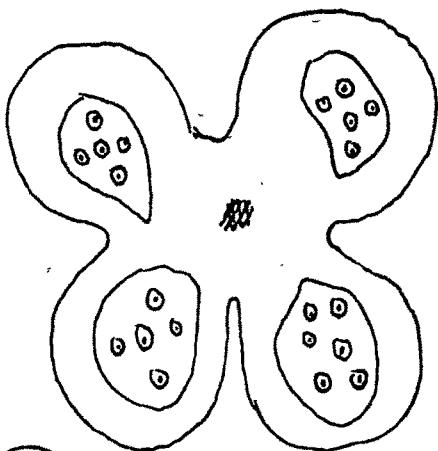
A₄



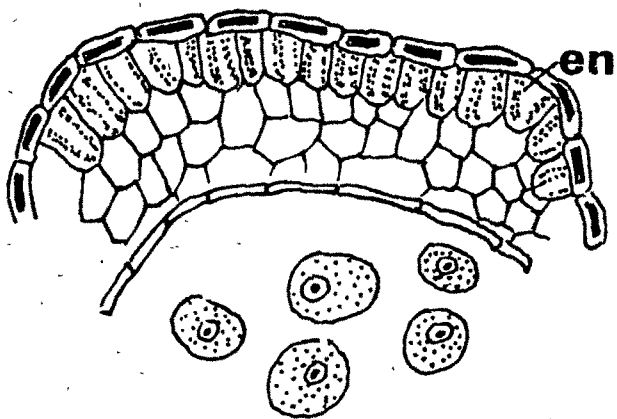
A₅



A₆



A₇



A₈

wall formation. The tetrad is tetrahedral and is enclosed in callose walls. As the tetrads separate into individual microspores, the callose in the walls are replaced by sporopollenin and simultaneously microspores enlarge. These microspores with their individual walls separate from each other and develop as pollen grains (Fig. 1.21F^(A₅, A₆)). The pollen nucleus divides to form a 2-celled pollen before dehiscence. The anther dehiscence is longitudinal and pollen grains are sticky.

3.2.1 Ultrastructure of the tapetum

Tapetum in C.roseus is glandular and secretory. It consists of a single layer of cells with its convex side facing the locular cavity (Fig. 1.22A). Two distinct stages can be recognised during their development and functioning. The first stage in which there is accumulation of osmiophilic droplets and synthesis of crystalloid protein and the second stage of elimination of the synthesized product into the cavity by the degeneration of the cells. The cytoplasm of the tapetal cell is rich in dilated rER, mitochondria, plastids, free ribosomes and few dictyosomes (Fig. 1.22, B). Of these, rER and plastids are very active as they show accumulation of protein crystalloids and osmiophilic droplets respectively.

Plastids are large with an electron dense matrix without any internal membrane system. They accumulate large number of osmiophilic droplets of varying electron density

from the early stages of the development of the tapetum (Figs.1.22 A-D; 1.23 A-C). Though these droplets show different electron density in the early stages, almost all of them become highly osmiophilic and show more or less similar electron opacity in later stages (Fig.1.23 A-C). Almost all the plastids which accumulate the osmiophilic materials are encircled either completely or partially by endoplasmic reticulum from the early stages of their development (Figs.1.22B, C; 1.23 B,C).

The most striking ultrastructural feature of the developing tapetum is the formation of protein bodies associated with the endoplasmic reticulum. The earliest visible indication in protein synthesis is the occurrence of high frequency of polysomes around the ER cisternae and in the cytoplasm (Fig.1.23 C,D). The rER cisternae becomes dilated and its lumen becomes electron dense (Fig.1.23 D). The dilated cisternae show aggregation of proteinaceous material (Fig.1.23D) and subsequently, the entire dilated cisternae becomes filled with typical crystalloid protein (Fig.1.24 A-D). The protein bodies show a regular lattice network which persists throughout the functioning stage of the tapetal cells (Fig.1.24 D). This high rate of protein synthesis is unique in the tapetal cells and not found elsewhere in the reproductive structures of C. roseus.

In the senescing stages, the tapetal cells show many distinct ultrastructural changes. The cytoplasm becomes electron translucent and the organelles especially ER and dictyosomes

disappear (Fig.1.25 A,B). Mitochondria, though showing degenerated appearance, persist till the last stage (Fig.1.25B). Proteins present, as crystalloid bodies in the early stages, lose their lattice appearance and become electron opaque cuneate crystals along with the degeneration of the ER (Figs.1.25A, 1.26 B). The plastid envelope disintegrates and the crystalloid protein mix with the osmiophilic droplets.

Subsequently, the cytoplasm becomes vesiculate, and the crystalline proteins get dispersed into fibrillar form (Fig. 1.25 B). Another notable feature in the senescing cells is the appearance of dark bodies along the periphery of the tapetal cells. These bodies, the Utrich bodies, have an overall electron - dense appearance with a prominent electron translucent middle region (Fig.1.25 C,D). Large osmiophilic droplets, along with the Utrich bodies, are released into the thecal cavity after the disintegration of the inner tangential wall of the tapetal cells. Cytoplasmic debris along with osmiophilic droplets and fibrillar dispersed protein are distributed in the thecal cavity (Fig.1.26 A-C).

3.2.2 Ultrastructure of the pollen grain and pollen tube

Pollen grain at the time of anthesis shows a prominent electron dense intine and a much demarcated darker exine (Fig.1.27 A). The cytoplasm is highly electron-dense and has many mitochondria and plastids (Fig.1.27 B). Most striking

feature of the pollen grain cytoplasm is the presence of large number of starch grains (Fig.1.27 B,C). During hydration, many of the starch grains develop cracks depicting their digestion or conversion into useful metabolites for facilitating germination.

The emerging pollen tubes have thin cell wall and a highly vesiculate cytoplasm (Fig.1.28 A). A cross section of the pollen tube just above its tip shows numerous mitochondria and highly hypertrophied dictyosomes (Fig.1.27 D). Cytoplasm also shows abundant large and small vesicles. The plasmalemma is smooth without much invagination at the early stage of germination.

The pollen tubes observed within the stylar tissue show many plastids with few internal membrane system (Fig.1.28 B). The cytoplasm has much branched abundantly distributed ER (Fig.1.29 A). The tubes at the tip show many dark bodies within the growing wall probably depicting the uptake of useful substances from the stylar secretions for the faster growth (Fig.1.28 C). The plasma membrane also shows, at some places, highly undulations containing many small vesiculate structures and fibrils presumably depicting membrane turnover (Fig.1.30 D). Cytoplasm also shows bundles of tubular structures, the nature of which is not known.

3.3 MEGASPORANGIUM

The ovule is anatropus, unitegmic and teneuinucellate borne on a parietal placenta. The integuments are initiated at an early stage and are well distinguished even at the archesporial initiation stage by the formation of distinct protuberance around the nucellar tissue. As the archesporial cell enlarges and divides, the integument grows rapidly and protrudes beyond the nucellus (Fig. 1.31 A).

3.3.1 Megasporogenesis

The hypodermal archesporial cell functions directly as the megaspore mother cell, without cutting any parietal cells (Fig. 1.31 A). The archesporial cell is flanked by 2 layers of cells laterally (Fig. 1.31 B). The archesporial cell elongates and divides transversely into ~~two~~ megaspore mother cells which further undergo simultaneous transverse division to form a linear tetrad (B_1, B_2, B_3, B_4). Of the four megaspores, both 1st and 2nd micropylar megaspores can be functional (B_5, B_6). The antipodals degenerate in the later stages (1.31C, D, B_5, B_6). The embryo sac is fully developed by stage II of flower development (B_7, B_8, B_9).

4. POLLEN GERMINATION STUDIES IN VITRO AND IN VIVO

4.1 IN VITRO POLLEN GERMINATION

Pollen grains from freshly dehisced anthers showed 90% germination in an optimum semi-solid medium containing 0.02%

Fig. B.

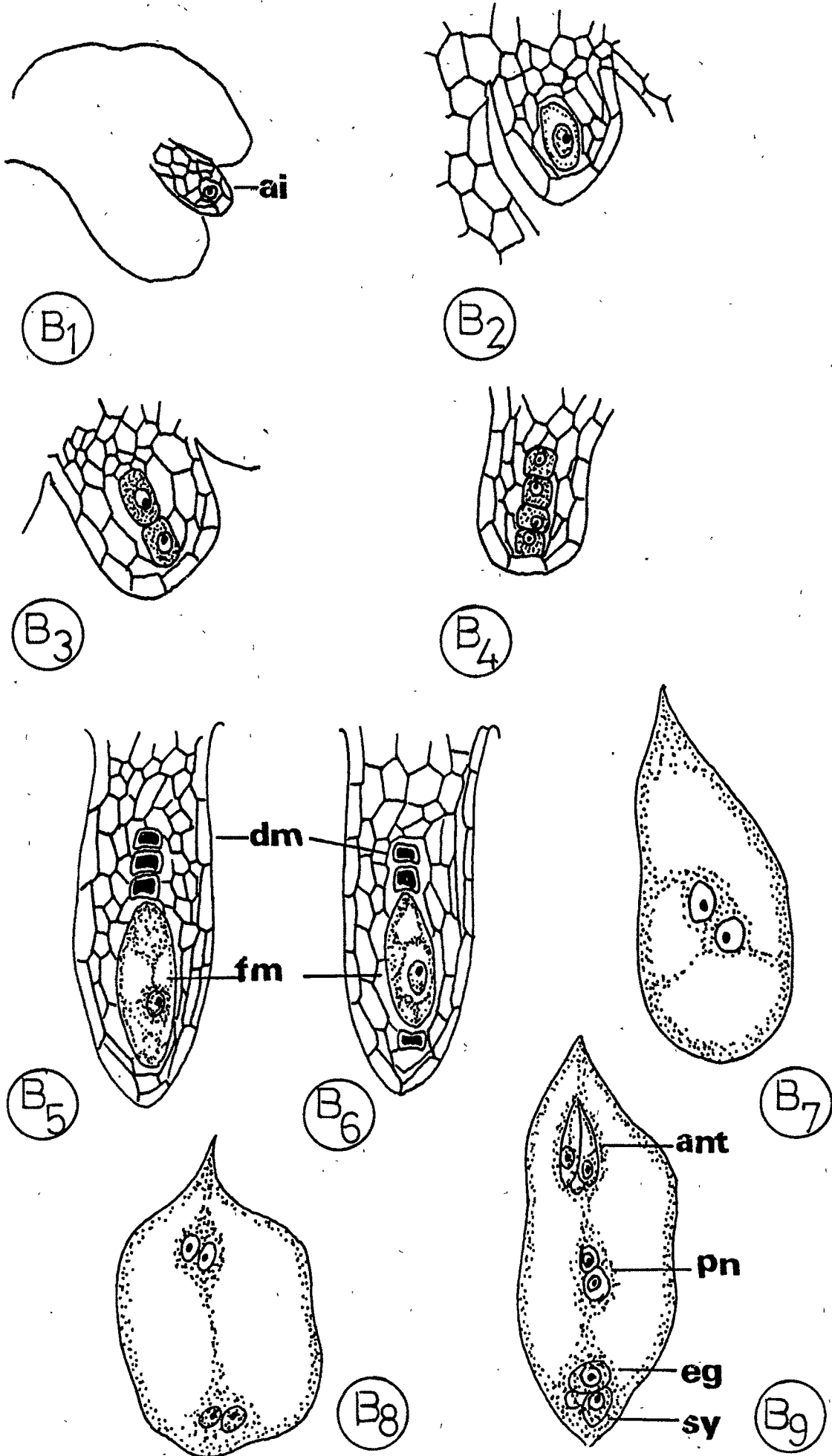
- B₁ - L.S. of ovule showing nucellar stage. X, 25
B₂ - Enlarged view of nucellus with archesporial initial. X, 50
B₃ - Nucellus showing dyad stage. X, 70
B₄ - Linear tetrad of megaspores. X, 70
B₅ - 1st functional megaspore. X, 100
B₆ - 2nd functional megaspore. X, 100
B₇ - Developing embryosac 2 celled stage. X, 50
B₈ - Developing embryosac 4 celled stage. X, 50
B₉ - 8 celled embryosac. X, 50

ai - archesporial initial; ant - antipodals; eg - egg;

dm - degenerating megaspores; fm - functional megaspore;

pn - polar nuclei; sy - synergids.

Fig-B



boric acid and 10% sucrose which is a modification of standard Brewbaker and Kwack's (1963) medium (Fig.II). The pollen tubes attained a length of 320 μ m in 120 mts time. For all further in vitro tests this medium with modified the concentrations were considered as the control.

4.2 EFFECT OF SELF AND CROSS PISTIL EXTRACTS ON IN VITRO POLLEN GERMINATION

Pollen germination percentage and tube length measured after the incorporation of self pistil and cross pistil extracts in to the nutrient medium showed an increase in pollen tube length in the case where the media was supplemented with self pistil extracts. However the percentage of germination did not show much variation.

TABLE 1

<u>Media</u>	<u>Tube length</u>	<u>Germination</u>
NM + cross pistil extract	308	85
NM + self pistil extract	346	85
Control	328	80

4.3 EFFECT OF SULPHUR DIOXIDE ON IN VITRO POLLEN GERMINATION

Pollen grains from freshly dehisced anthers when dusted on semi-solid nutrient medium and exposed to varying concentrations of sulphur dioxide showed considerable decrease in the percentage of germination as well as in the

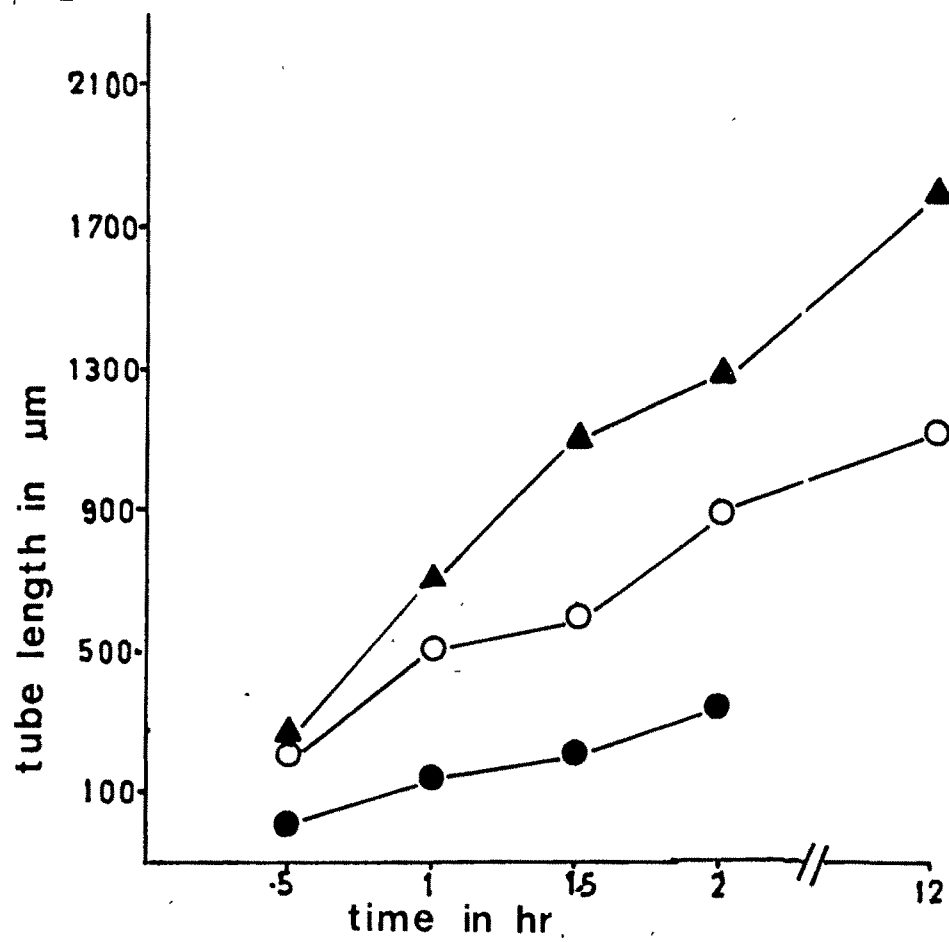


Fig. II. Graph representing in vitro and in vivo pollen germination in C. roseus.
In vitro (●-●); Cross pollination (○-○);
 Self pollination (▲-▲).

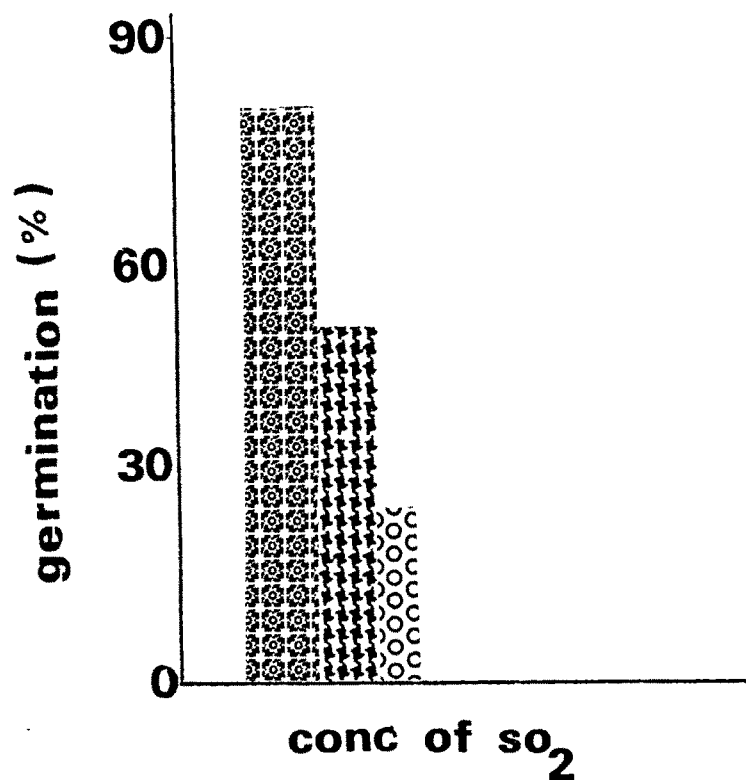


Fig. III. Histogram depicting the effect of SO₂ on in vitro pollen germination in C. roseus. Control (■); 0.5 ppm (▨); 1 ppm (○).

tube length. At 0.5 ppm SO₂, the percentage of germination was reduced to 40% and the tube length reached 126 μ m in 120 mts time (Fig. III). At 1 ppm SO₂, the percentage germination was further lowered to 20% and the length of the tube reached 50 μ m in the same duration of time. There was total inhibition of pollen germination at 1.5 ppm of SO₂.

4.4 EFFECT OF SO₂ ON IN VIVO POLLEN GERMINATION

While there was considerable difference in the percentage of germination and tube length in vitro compared to the control, the in vivo results indicated only a slight decline in tube length. However, percentage of germination was not seriously affected. Maximum reduction in percentage of germination and tube length was observed in the case were both pistil and the pollen were exposed to sulphur dioxide prior to pollination. Results of the various pollinations are indicated (Table 2).

4.5 EFFECT OF SPERMIDINE AND MGBG ON IN VITRO POLLEN GERMINATION AND TUBE GROWTH

Pollen grains from freshly dehisced anthers were germinated in the nutrient medium supplemented with various concentrations of spermidine or MGBG or actinomycin-D alone or in combination. Among the various concentrations of spermidine tested, 10⁻⁶ M and 10⁻⁵ M enhanced tube growth while 10⁻⁴ M reduced tube growth (Table 3) MGBG at 0.5 x 10⁻³

TABLE - 2Effect of SO₂ on pollen germination in vivo in C. roseus

Conc. of SO ₂ (in ppm)	Time (in mts.)	Type of Pollination	% of germinat- ion	Tube length
0.5	120	TS x NP	65	85
0.5	120	TP x NS	65	105
0.5	120	TP x TS	20	18
1	120	TS x NP	30	48
1	120	NS x TP	40	55
1	120	TP x TS	20	15
1.5	120	TS x NP	5	10
1.5	120	TP x NS	10	20
1.5	120	TP x TS	5	10
Control	120	NP x NS	80	280

The values are the mean of 10 observations.

TS : Treated stigma, TP : Treated pollen, NS : Normal stigma,
NP : Normal pollen.

10^{-3} and 1×10^{-3} M reduced both percentage germination and tube growth. A total inhibition of pollen germination was observed with 1.5×10^{-3} M MGBG (Table 3) and the pollen grains showed bursting at the germ pore liberating the contents. Pollen grains when transferred to the medium containing 10^{-6} and 10^{-5} M spermidine, gave 68 % and 81% germination recovery respectively with considerable tube growth. Further pollen tube growth was markedly reduced when 1.5×10^{-3} M MGBG was incorporated into the nutrient medium after 60 mts of incubation (Table 3).

Experiments using actinomycin-D indicated a total reduction in the percentage of germination and tube growth compared to the control, even after the incorporation of spermidine at 10^{-5} M concentration. However, there was complete inhibition of pollen germination at higher concentration of actinomycin-D (10^{-6} & 10^{-5}) along with spermidine at 10^{-5} M. Actinomycin-D incorporated alone into the nutrient medium revealed a further decrease in the percentage of germination and tube growth. (Table 4)

4.6 - IN VIVO POLLEN GERMINATION

Pollination carried out using cross and self pollen indicated that C.roseus is self compatible. Self pollen showed maximum germination in a period of 120 mts (Fig.1.32 A). The pollen tubes reach the base of the stigma head in about 4 h and the base of the style in about 8 h. Self pollination at

TABLE - 3

Effect of MGBG and spermidine (SPD) on pollen germination and tube length in Catharanthus roseus

Treatments	Germination (%)	Tube length (μm)
Experiment 1		
Control (nutrient medium)	95 \pm 2.2	301 \pm 5.4
0.5 x 10 ⁻³ M MGBG	67 \pm 3.2	134 \pm 5.9
1.0 X 10 ⁻³ M MGBG	10 \pm 0.4	43 \pm 1.6
1.5 x 10 ⁻³ M MGBG	0.0	0.0
Experiment 2		
1.5 x 10 ⁻³ M MGBG	0.0	0.0
10 ⁻⁶ M SPD	68 \pm 3.3	104 \pm 3.7
10 ⁻⁵ M SPD	81 \pm 3.0	238 \pm 3.5
10 ⁻⁶ M SPD*	95 \pm 1.2	331 \pm 4.5
10 ⁻⁵ M SPD*	97 \pm 1.4	353 \pm 4.9
Experiment 3		
1.5 x 10 ⁻³ M MGBG	96 \pm 1.0	231 \pm 3.8

Expt. 1. Pollen grains germinated for 120 min. in nutrient medium containing different concentrations of MGBG.

Expt. 2. Pollen grains incubated in nutrient medium containing 1.5x10⁻³ M MGBG for 30 min were transferred to the medium with different concentrations of SPD. Control (*), pollen grains incubated in nutrient medium for 30 min were transferred to the medium containing different concentrations of SPD.

Expt. 3. MGBG was added to the nutrient medium after 60 min of incubation.

Figures are the mean values of five experiments \pm s.e. At least 30 determinations were made for each experiment. Observations were made after 120 min of incubation.

TABLE - 4

Effect of spermidine (SPD) and actinomycin-D (Ac-D) on pollen germination and tube length in C. roseus

Treatments	Germination (%)	Tube length (μM)
Experiment		
Control (nutrient medium)	96 \pm 1.3	3.9 \pm 6.4
Control \pm 10 ⁻⁵ M SPD	98 \pm 1.9	380 \pm 3.6
Control + 10 ⁻⁵ M SPD + 10 ⁻⁹ M Ac-D	82 \pm 2.4	114 \pm 2.2
Control + 10 ⁻⁵ M SPD + 10 ⁻⁸ M Ac-D	54 \pm 1.7	109 \pm 2.0
Control + 10 ⁻⁵ M SPD + 10 ⁻⁷ M Ac-D	38 \pm 1.5	64 \pm 1.1
Control + 10 ⁻⁵ M SPD + 10 ⁻⁶ M Ac-D	0.0	0.0
Control + 10 ⁻⁵ M SPD + 10 ⁻⁵ M Ac-D	0.0	0.0
Control + 10 ⁻⁹ M Ac-D	78 \pm 1.3	112 \pm 1.8
Control + 10 ⁻⁸ M Ac-D	59 \pm 1.9	101 \pm 1.6
Control + 10 ⁻⁷ M Ac-D	34 \pm 1.1	68 \pm 1.9
Control + 10 ⁻⁶ M Ac-D	0.0	0.0
Control + 10 ⁻⁵ M Ac-D	0.0	0.0

Figures are the mean values of five experiments \pm s.e. At least 30 determinations were made for each experiment. (Observations were made after 120 min of incubation).

various stages of the stigma development showed that stigma is receptive from stage II (Fig. IV). The pollen grains landing on the stigma get hydrated and germinate in the exudate present on the stigmatic head and enter through the lateral sides of the dumb-bell shaped stigma (Fig. 1.32 B-E).

The pollen tube entry is exclusively through the lateral side of the stigma and they grow among the loosely arranged cells on the lateral side of the stigmatic head. The pollen tubes from the pollen grains, germinating on the upper portion of the stigmatic head grow among the papillae cells and reach the lateral basal side of the stigma to effect the penetration (Fig. E). No pollen grain penetrates the stigmatic cell at the upper region. The pollen tubes grow in the intercellular spaces of the style. Pollen grains falling inside the stigmatic flap also germinate and enter the style through the junction of the stigma and style, since the transmitting tissue extends to the periphery (Fig. 1.32 E). In the style, the pollen tube grows among the transmitting tissue and reaches the ovary. Bud pollination showed pollen germination in all stages of stigma development except at stage I. Self pollination however revealed maximum pollen germination (Fig. IV).

In cross pollination, the pollen germinates on the stigma and penetrates the stigma tissue, but were inhibited

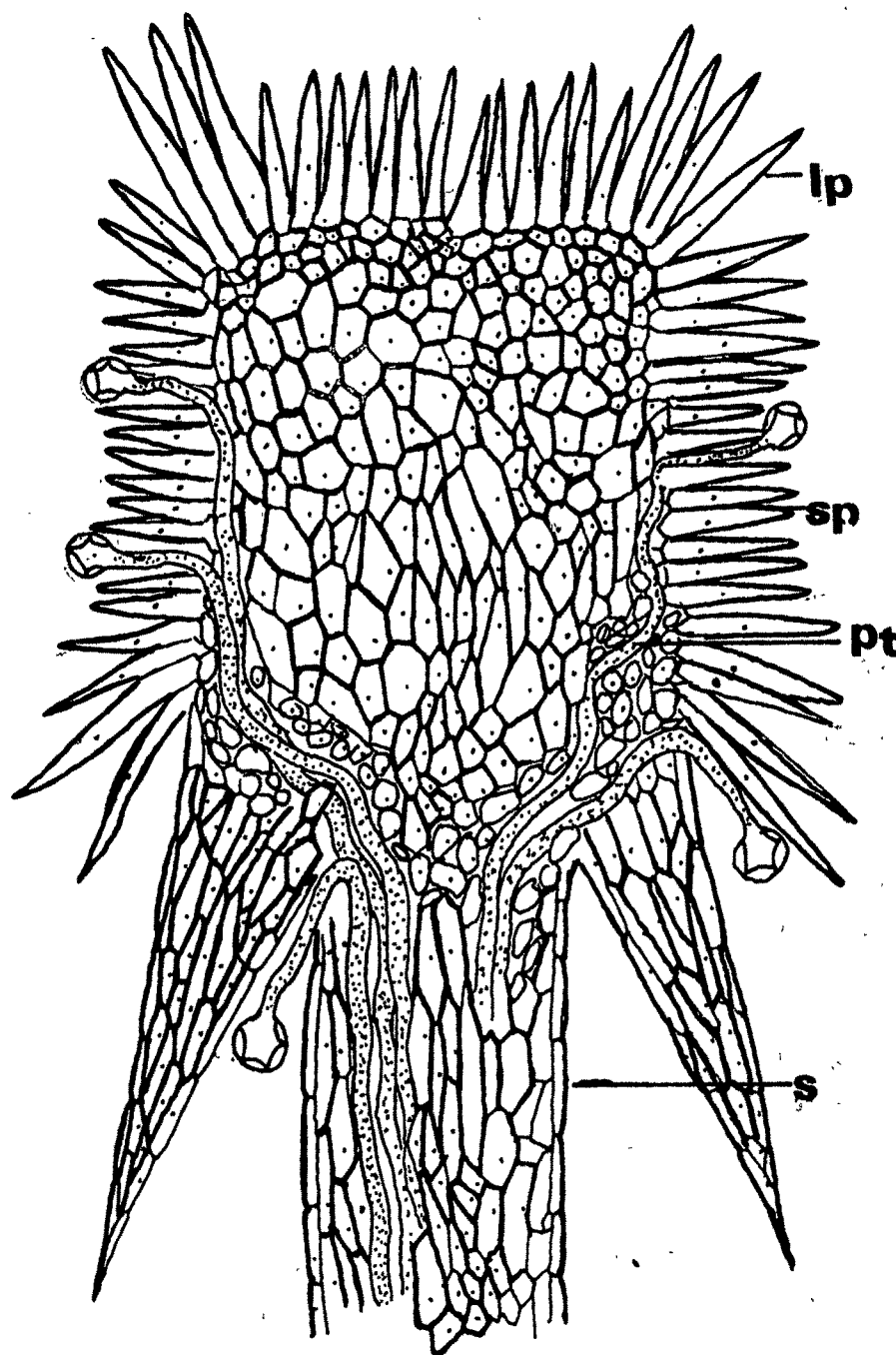
Fig. E -

Fig. Diagrammatic representation showing the possible mode of entry of pollen tubes in to the style in C. roseus. The pollen tubes in this plant enter exclusively through the basal region of the stigma. The pollen grain germinated in the stigmatic exudate at the lateral side, grow between the papillae cells down, till the flap and penetrate the loosely packed cells present and reach the transmitting tissue of the style. No pollen tube was observed at the upper massive region of the dump-bell shaped stigma.

lp - long papillae ; pt - pollen tube ; s - style ;

sp - short papillae .

Fig. E



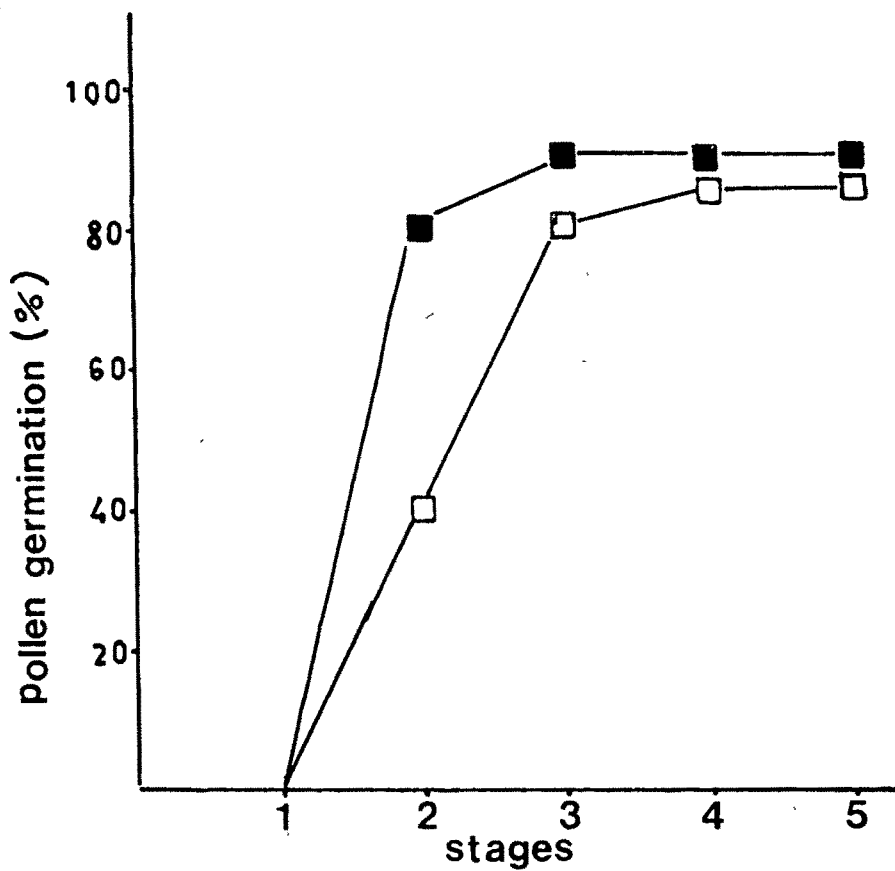


Fig. IV. Graph representing the results of bud pollination in C. roseus.
Self pollination (■); Cross pollination (□).

at the tube tip (Fig.1.32 F). Few pollen grains were observed inhibited on the stigma surface itself and no germination occurred (Fig.1.32 G).

4.7 POLLEN VIABILITY AT DIFFERENT STORAGE CONDITIONS

Retention of pollen viability was checked at various storage conditions. Results are plotted in a graph (Fig. V). Maximum pollen viability was retained for about 10 days in the case where pollen were stored at -4°C . At room temperature the viability was found to be lost in 4 days.

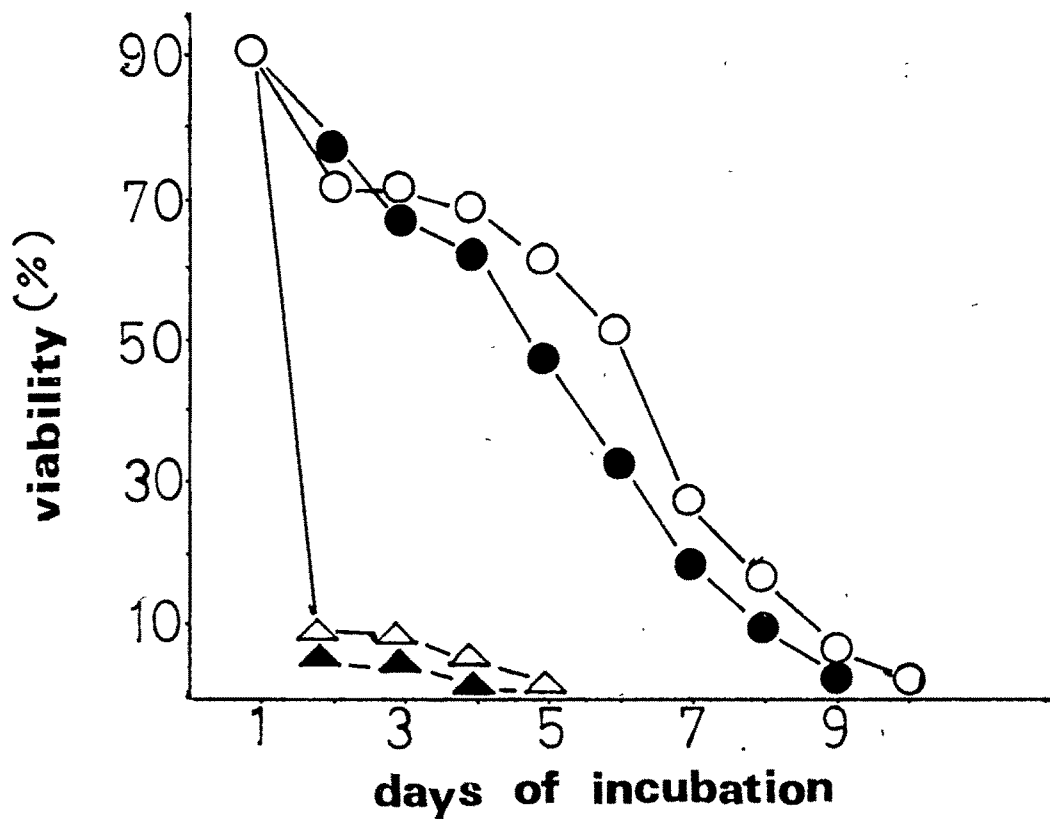


Fig. V. Graph showing viability percentage of pollen at different storage conditions. in C. roseus.

-4°C (O-O); 4°C (●-●) dessicated condition (◄-►);
Room temperature (▲-▲).

1. GENERAL DESCRIPTION OF THE PLANT

Withania somnifera Dunal (Solanaceae) is an erect perennial herb growing wild in dry regions. The stem is cylindrical, branched, solid, covered with glandular uniseriate branched or unbranched hairs, Leaves cauline and ramal, exstipulate petiolate; petiole hairy, alternate sometimes opposite. The leaves at a node are unequal i.e. one is always larger than the other. Simple leaves are ovate, entire, acute, covered with glandular as well as branched hairs especially on the midrib, reticulate, subsessile, Pedicel is hairy and ebracteolate. Flowers actinomorphic, bisexual, hypogynous, tetracylic, small, greenish yellow and not scented. Calyx five, fused, companulate, valvate, hairy, persistent and becoming urceolate in fruit green and inferior, Corolla five, fused campanulate; corolla tube only slightly longer than calyx, valvate, greenish yellow and inferior. The corolla lobes become reflexed at their tips. The whole corolla tube may fall down in mature flowers (caducous). Stamens five, free epipetalous, inserted near the base of the corolla tube. Filaments unequal in length, anthers bithecous, basifixed, oblong, dehiscence longitudinal, introse. Gynoecium bicarpellary, trilocular (at certain places) by the formation of a false septum. Ovules many, placentation axile, placenta swollen, ovary obliquely placed, hairy, seated on an orange coloured and bilobed nectar secreting disc. Style simple, longer than the stamen, stigma bifid, papillate and green. Fruit is yellow

or red berry, green when immature, enveloped by persistent calyx. Seed is endospermous.

1.1 ECONOMIC IMPORTANCE

Withania somnifera is used in India as a sedative. Studies have shown that Withania contains a dozen biochemically heterogenous alkaloids, like withanin, tropine, psuedotropine, hygrine, anaferin, and anahygrine. The principle responsible for the sedative action of the drug has not yet been determined but the study of the alkaloids has advanced our knowledge of chemical and taxonomic relationships of solanaceous plants.

2. PISTIL

2.1 STIGMA

Mature stigma of W. somnifera is bilobed, reflexed and funnel shaped with a central depression, (Fig.2.1 C,D) and is of wet type. The exudate is scanty and is confined in between the loosely arranged papillae cells. It is evident only by the glistening nature of the stigma at the receptive stage. The stigma consists of elongated multicellular highly vacuolated and loosely arranged papillae cells. Each papillae has a distinct cuticle. The papilla cells at the central depression is continuous with the transmitting tissue of the style.

Stigma at stage I is distinctly bilobed (Fig.2.2A) and consists of a homogenous mass of cells. The stigma surface is

uneven with a slight depression at the centre (Fig.2.2B). By stage II, the epidermal cells elongate and bulge forming dumb-bell shaped papillae initials. These initials are slightly vacuolated with abundant lipid droplets (Fig.2.2C,D). The pistil at stage III shows an elongated style and an expanded stigma (Fig.2.2B). The papillae cells become loosely arranged and glandular, and the lipophilic material fills the intercellular spaces by stage IV (Fig.2.2F,G). By stage V the papillae become highly elongated densely stained and shows degeneration. The bifid nature becomes more pronounced as the central depression becomes more prominent (Fig.2.2H). The cells at the centre of the depression are highly vacuolated and do not show degeneration while those on the sides of the depression show senescence.

2.1.1 Ultrastructure of the stigma

The stigma of W. somnifera at the receptive stage show only sparse sticky exudate which is not free flowing, and is exclusively present above the papillae cells and also within the intercellular spaces of the subpapillae and the transmitting tissue. The papillae cells are multicellular, uniseriate and are distributed only on the surface of the stigma head. They are connected to the bulk of the stigma through sub-papillae cells which are also glandular and take active part in secretion.

The papillae cells have thin cell walls with compactly arranged microfibrils (Fig.2.3 A,B). The radial wall between the cells are usually thinner than the tangential walls and contain many plasmodesmata connections (Fig.2.3A,B, arrow). Cuticle is thin, spread over the entire surface of the papillae cells. Above the cuticular layer there is a thin uniform deposition of electron dense material which contains many vesicular structures and osmiophilic droplets. This layer, the pellicle, covers the entire surface of the papillae cells (Fig.2.3 A,B, arrow heads). However, when the papillae cells are close together, the entire intercellular space becomes filled with secretory materials, still maintaining the intactness of the pellicle. (Fig.2.3A). This unique appearance of the secretory material between the papillae cells is the only indication of free flowing exudate on the stigma surface.

The cytoplasm of the papillae cells at the secretion stage is highly electron dense, contains osmiophilic droplets, and many large vacuoles with osmiophilic materials filling the vacuolar space (Figs.2.3A,B; 2.4 A,B;2.5 A,B). The vacuoles show coalescence, which lead to the formation of large vacuoles completely filled with osmiophilic material. Osmiophilic material is seen traversing the tonoplast into the vacuoles in most of the cells (Figs.2.3B,2.4A,B). In the late secretory phase, many cells show large vacuoles filled with secretory material compared to the coalescing

small vacuoles in the cells at the early secretory phase (Compare Figs.2.3A,B; 2.4 A with Fig.2.5A,B).

Nucleus is prominent in the papillae cells having mostly spherical or oval shapes containing dispersed and condensed chromatin (Figs.2.3A,B; 2.4A, 2.5 B). The most prominent organelle in the cytoplasm is the plastid. They are mostly crowded near the nuclei and are highly electron-dense (Fig.2.3A,B). Plastids show various shapes ranging from spherical, oval, fusiform and ring shapes. Most of them do not contain a well defined membrane system, however, some of them have well developed thylakoids (Figs 2.5B; 2.6A; 2.7B, C, D; 2.8 B,C). The thylakoids show moderate stacking, forming small grana, linked by intergranal lamellae (Figs.2.7B, 2.8A). The most striking feature, depicting their active role in secretion is the accumulation of large osmiophilic droplets (Fig.2.7A). Some of them fill almost the entire lumen of the plastids or chloroplasts (Figs.2.7D; 2.8 B,C). In fact, this structural feature makes the lumen of the plastids highly electron dense masking the other details of the lumen (Fig.2.3 A,B). Some of the plastids are encircled either partially or completely by endoplasmic reticulum (Figs 2.6A, 2.7A,C).

Mitochondria which are smaller compared to the plastids are also many, distributed randomly in the cytoplasm (Figs.2.3A, 2.4B, 2.5A,B). They have well developed tubular

crisetae and do not show any association with the secretory material (Fig.2.5A), and presumably are not directly involved in the synthesis of secretory material. Some of them in the late stage of secretion (Stage V) show loss of crisetae and patches of electron translucent areas (Fig.2.6C). Endoplasmic reticulum is usually rough (Fig.2.9A), though smooth ER is also seen rarely (Fig.2.8 D). They show close association with the plasmalemma (Figs.2.7B, 2.9 A) and also with multivesicular bodies (Fig.2.9C). Dictyosomes in the cytoplasm comprise of ² few tubular cisternae stacked compactly together giving a highly electron dense appearance (Figs.2.4B, 2.5 A; 2.6 A,B). Vesicles, which are devoid of any contents originate from them (Fig.2.6A). Sometimes, small vesicles or multivesicular bodies are also seen at the vicinity of the dictyosomes (Fig.2.6B). Multivesicular bodies containing electron dense material or vesicles containing multilamellate structures are also frequent in the cytoplasm of some of the papillae cells (Fig.2.5A,B, arrows). The vacuoles in the sub-papillae cells show accumulation of phenolic materials and small dark globules are seen traversing the tonoplast (Fig.2.6C).

Another striking feature of the stigma of W. somnifera is the deposition and accumulation of osmiophilic, secretory material in the intercellular spaces between the papillae and sub-papillae cells (Figs.2.7A,B; 2.8A,D; 2.9A,B). These

materials accumulate as large droplets amidst the cellulosic microfibrils. This may be to facilitate the growth of the pollen tubes, which normally will have to penetrate the intercellular spaces of sub-papillae and the cells below them to reach the transmitting tissue. In some cases, small irregular vesicles varying fibrillar and small highly electron dense droplets are released in to the intercellular spaces (Fig.2.9B, arrows)

In the post-pollination stage of the stigma, the papillae cells show degeneration compared to the sub-papillae (Fig.2.10A). The first indication of degeneration is the loss of contents of the cytoplasm and degeneration of mitochondria and plastids (Fig.2.10C). Mitochondria and plastids loose their membrane system while, the ER forms stacks. In the late senescent phase, the cytoplasm contains persisting ribosomes and degenerated organelles (Fig.2.10A,B). However, the most unique character is the persistence of pellicle as an intact layer covering the papillae cell wall (Fig.2.10A). The free exudate, which was present in the spaces between the papillae cells dissappeared at this stage.

2.2 STYLE

The style is solid type and consists of three distinct zones namely the epidermis, cortex and a central transmitting

tissue (Fig.2.11A). Two distinct vascular bundles flank the transmitting tissue throughout the length of the style and extends up to the stigmatic head (Fig.2.11B). The transmitting tissue consists of loosely arranged elongated parenchyma cells which are rich in cytoplasm and moderately vacuolated with intercellular spaces filled with secretory substances. The epidermis of the style has a distinct cuticular lining (Figs.2.11C, 2.11D).

2.2.1 Ultrastructure of the transmitting tissue

The cells of the transmitting tissue are long with blunt or tapering end walls (Fig.2.12A). Some of the cells are highly vacuolate, while others have dense cytoplasm with small coalescing vacuoles. They have thin cell wall with little or no intercellular spaces in the early stage of the style development (Stage III). The cell wall at certain regions show thickened appearance, presumably because of the loosening and swelling of the middle lamella (Fig.2.12A, arrows).

Nucleus is oval or fusiform with uniformly distributed chromatin. However, along the nuclear membrane condensed chromatin is also seen (Fig.2.12A, arrowheads). Vacuoles contain dark bodies as well as fibrillar material. The cytoplasm also shows small vesicles without any content. Dark, highly electron dense plastids of different shapes are prominent in the cytoplasm. Some of the plastids contain

electron transparent areas in the lumen. Few of them also show typical chloroplast structure (Fig.2.12B). Mitochondria are small with few internal membrane, while endoplasmic reticulum is rough, distributed randomly in the cytoplasm.

Towards the receptive stage of the stigma, the cytoplasm accumulates large osmiophilic droplets near the highly stacked rough ER (Fig.2.12B). The middle lamella loosens and lot of osmiophilic secretory material becomes deposited in the middle lamella region as well as in the intercellular spaces (Fig.2.12 C). Vesicles containing fibrillar material **are** also seen within the secreted material (Fig.2.12B, arrows). At the receptive stage, the cytoplasm becomes highly vacuolate and the vacuoles contain abundant phenolic material.

2.3 HISTOCHEMISTRY OF THE STIGMA AND STYLE

The exudate is insoluble in water and completely soluble in chloroform/methanol. It stains intensely for lipids, in all stages of stigma development when stained with Auromine O (Fig.2.13A). Sudan IV staining is less intense in the exudate whereas, the cuticle is distinctly stained both with Sudan IV and Auromine O (Fig.2.13E,F). Auromine O staining shows an intact cuticle in the younger stages of papillae cells, whereas in the mature stages, the cuticle is discontinuous (Fig.2.13C,D).

The papillae cell stains intensely for insoluble polysaccharides from IV stage onwards. ^(2.13 E) Abundant starch

deposits are evident in the transmitting tissue and cortical cells at stage IV (Fig.2.13C). Later stages show the depletion of starch deposition in both cortical cells and transmitting tissue. There is a high total protein content in the papillae cells in all stages of stigma development. A distinct pellicle is evident over the papillae cells from stage IV onwards (Fig.2.13D). However, biochemical estimation of stigma and stylar extract showed a gradual increase in protein content which is maximum at stage III (Fig.VI).

2.4 ENZYME CYTOCHEMISTRY OF STIGMA

Non-specific esterase

Stages I and II of stigma development show moderate activity for non-specific esterase in the papillae cell cytoplasm. From stage III onwards, the distinct pellicle shows intense activity of non-specific esterase. The exudate accumulating in between the cuticle-pellicle layer also stain intensely for non-specific esterase. In mature papillae cell, the activity is undetectable in its cytoplasm (Fig.2.14A).

Peroxidase

Peroxidase activity is intense at stages II and III and show meagre to moderate activity in later stages in the cytoplasm of the papillae cell (Fig. 2.14B).

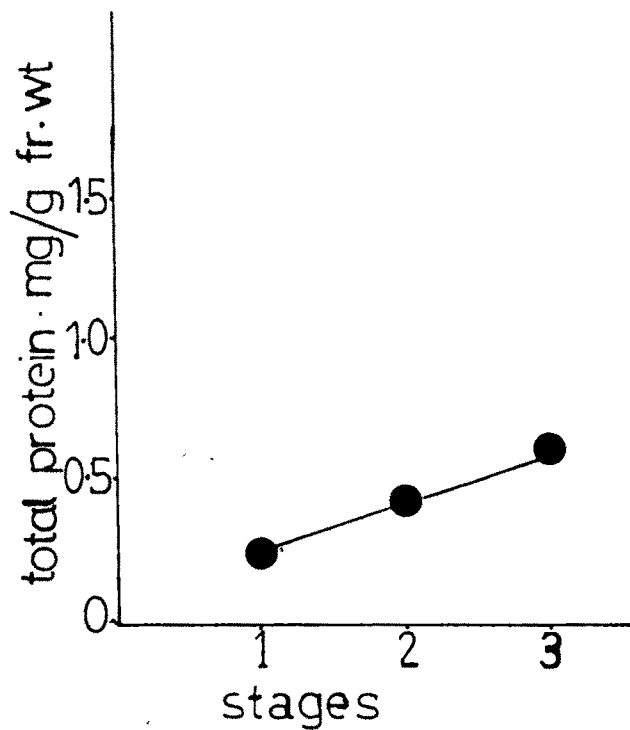


Fig. VI. Graph representing total proteins in the stigma/stylar extracts at different stages in W. somnifera.

Stage 1 - (Early bud ~~late~~ bud)

Stage 2 - (Early anthesis)

Stage 3 - (Anthesis and late anthesis).

Succinate dehydrogenase

Succinate dehydrogenase shows intense activity in the papillae cells at stages III & IV. The sites of activity were confined mainly towards the base of the papillae cell. Stages I & II showed moderate activity (Fig.2.14C).

Acid phosphatase

Stages I & II of stigma development showed meagre acid phosphatase activity in the papillae cell. The activity was intense during the later stages. The pellicle also shows intense reaction for acid phosphatases (Fig.2.14D).

Adenosine triphosphatase

The papillae cells at stages II, III & IV showed moderate wall bound activity for adenosine triphosphatase. The pellicle also showed moderate activity of ATPase (Fig.2.14E,).

3. MICROSPOROGENESIS AND MEGASPOROGENESIS

3.1 Anther

Mature anther is bithecous and tetrasporangiate. Each microsporangium consists of an outer epidermis and a double to multilayered endothecium, single middle layer and a single layered tapetum which is secretory (Fig.2.15A,B).

3.2 MICROSPORANGIUM AND MICROSPOROGENESIS

The microsporangium consist of homogenous mass of cells surrounded by an epidermis. It becomes four lobed and a plate

of archesporial initials gets differentiated in each lobe (Fig. C₁). They undergo periclinal divisions to form primary parietal cells and primary sporogenous cells^(C₂). The primary parietal cells later give rise to inner and outer secondary parietal cells. The inner secondary parietal cells give rise to tapetum whereas the outer secondary parietal cells form a double layered endothecium and middle layer (Fig. 2.15A, B, C, D; C₃, C₄). The tapetal cells are irregularly layered, rectangular and uninucleate. The microspore mother cell occupies a central position and the fully formed microsporangium shows the tapetal cells pushed to the periphery (Fig. 2.15E, F; 2.16A, B; C₅, C₆). The tapetum persists even up to the late stage and therefore is of the secretory type.

3.2.1 Microsporogenesis

The primary sporogenous cells divide repeatedly to form the microspore mother cell. The first meiotic division is followed by wall formation thus having a simultaneous type of cytokinesis. Both tetrahedral and isobilateral tetrads are present. The microspores with their individual walls separate from each other and develop as pollen grains (Fig. 2.15E, F; 2.16A, B). The pollen nucleus divides to form two celled pollen before anther dehiscence. The pollen grains are liberated by the longitudinal dehiscence of the anther (Fig. 2.16C, D, E, F).

Fig. C.

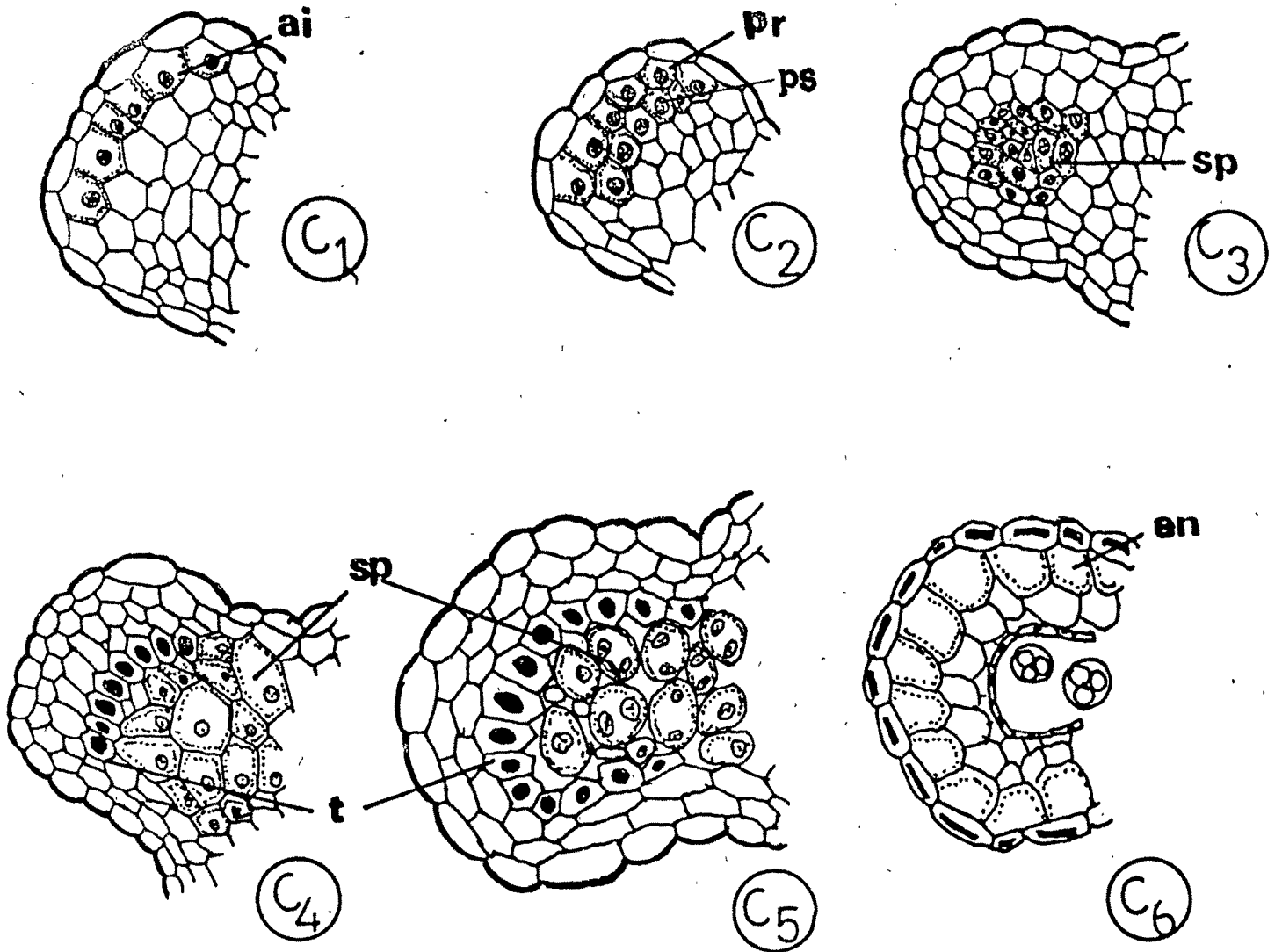
- C₁ - Anther lobe showing single hypodermal layer of archesporial tissue. X,50
- C₂ - Archesporial tissue divided in to a primary parietal layer and primary sporogenous layer. X,25
- C₃ - Anther lobe showing primary parietal cell dividing to form secondary parietal cell. X,50
- C₄ - Sporogenous cell divide repeatedly to form a mass of sporogenous cells. X, 50
- C₅ - Anther lobe showing single mass of spore mother cells with a distinct tapetal layer. X,100
- C₆ - Mature anther lobe showing epidermal layer, endothelial layer with distinct fibrous thickening intact tapetum, and pollen grains. X,50

ai - archesporial initial; en - endothecium

ps - primary parietal layer; sp - secondary parietal layer

sp - sporogenous cell; t - tapetum.

Fig. C



3.2.2 Ultrastructure of the pollen grain and pollen tube

The pollen grains of W. somnifera show a uniformly dense intine and a highly electron dense exine (Fig.2.17A). The exine is clearly differentiated into a nonsculptured nexine and a highly ornamented sexine (Fig.2.17A,B). The sculptured regions of the exine shows osmiophilic material covering the surface as well as within the ornamentations.

The cytoplasm is highly vesiculate. The vesicles originate from the highly active dictyosomes which are abundant in the cytoplasm (Fig.2.17A). Plastids are few with no internal membranes. Mitochondria are abundantly distributed near the plasmalemma and have profuse cristae (Fig.2.17A,B,C). Endoplasmic reticulum, both smooth and rough, is distributed randomly in the pollen cytoplasm.

The pollen tube shows a highly dispersed microfibrillar texture in its cell wall (Fig.2.18A). The cytoplasm is dense with abundant mitochondria, dictyosomes, smooth and rough ER, and profuse vesicles (Fig.2.18B). The pollen tube tip shows dictyosomes producing large vesicles (Fig.2.18B), while at the middle region, they produce small minute vesicles (Fig.2.18C). The large vesicles show fusion (Fig.2.18B). The smaller vesicles usually associate into multivesicular bodies (Fig.2.18C arrows). The pollen tube tip also shows concentric membrane structures probably depicting a high membrane turn

over (Fig.2.18B). Cross sectional view of the stigma sub-papillae and the cells below them show pollen tubes penetrating the intercellular spaces (Fig.2.19A,B). The penetrating tubes show a wavy, thin cell wall with an undulated plasmalemma. The intercellular spaces show the secretory material which surrounds the growing tube (Fig.2.19A,B). The cytoplasm is highly vesiculate and contain numerous mitochondria, dictyosomes, smooth and rough ER (Fig.2.19B).

3.3 MEGASPORANGIUM

The ovule is anatropous, unitegmic, borne on axile placenta. The nucellus is single layered and is exposed in the early stages. The integument development is slow and is evident only at the linear tetrad stage.

3.3.1 Megasporogenesis

From the hypodermal mass of cells a single archesporial cell gets differentiated and functions as the megaspore mother cell. This is flanked by two layers of cells on the lateral side (Fig.2.20A, D1 D2). The megaspore mother cell enlarges and divides to form two cells which undergo simultaneous division to form a linear tetrad (D3). Of the four megaspores, the megaspore at the chalazal end is functional. The female gametophyte is of the polygonum type. Besides, the embryosac has a distinct endothelial lining (Fig.2.20B,C,D). The

Fig. D.

- D₁ - L.S. of ovule showing nucellar stage. X, 25
- D₂ - Enlarged view of nucellus with archesporial initial. X, 50
- D₃ - Dyad stage. X, 50
- D₄ - Linear tetrad stage. X, 35
- D₅ - 2nd functional megaspore. X, 50
- D₆ - Developing embryo sac. 2 celled stage. X, 50
- D₇ - Developing embryo sac. 4 celled stage. X, 50
- D₈ - 8 celled embryo sac. X, 50

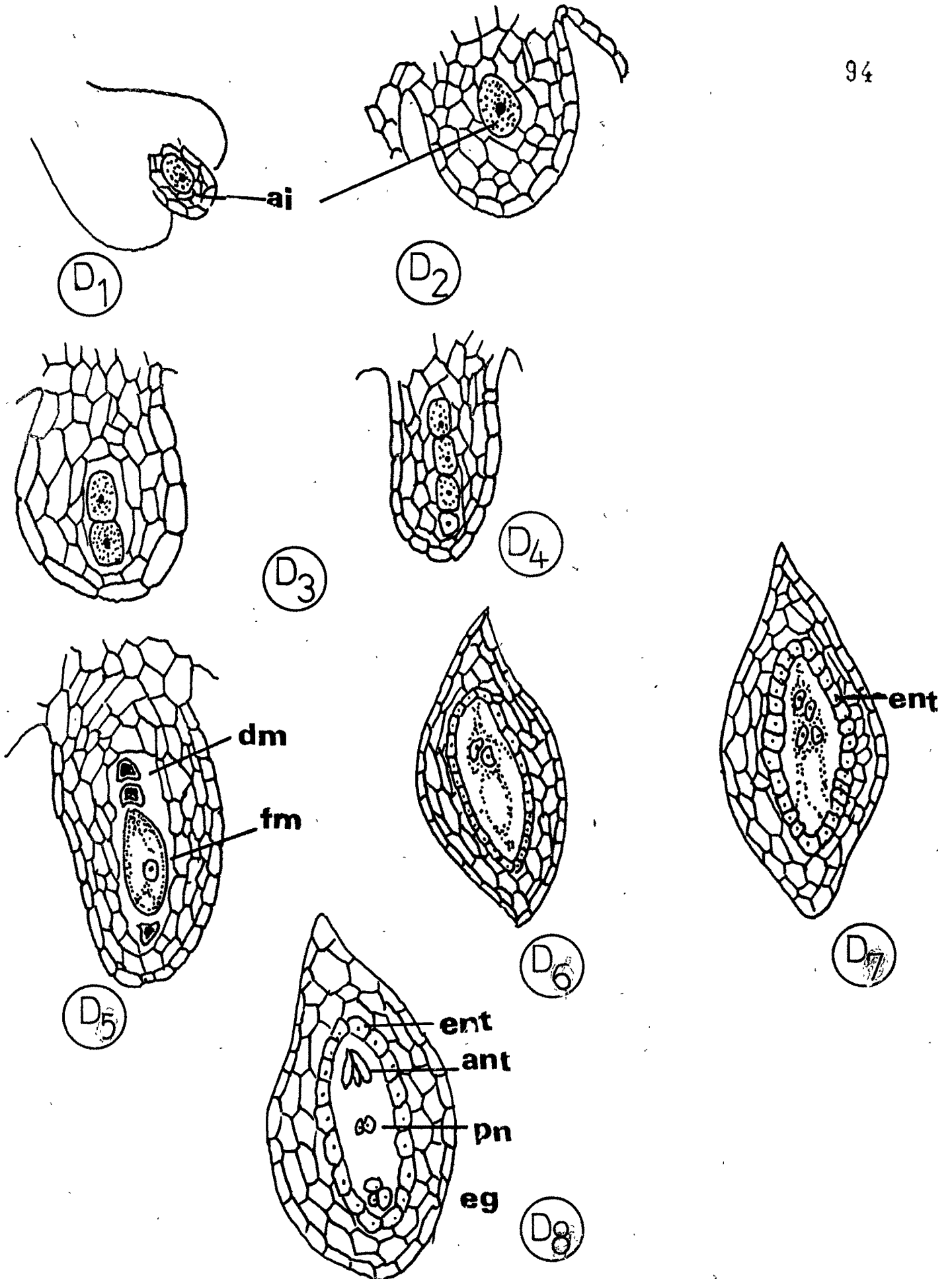
ai - archesporial initial; ant - antipodals;

eg - egg apparatus; ent - endothelium;

dm - degenerating megaspores; fm - functional megaspore

pn - polar nuclei.

Fig - D



antipodals persist till the later stage of embryosac development (Fig.2.20 E,F; D₄-D₉).

4. POLLEN GERMINATION STUDIES IN VITRO AND IN VIVO

4.1 IN VITRO POLLEN GERMINATION

Pollen grains from freshly dehisced anthers showed 85 % germination in an optimum semisolid medium containing 0.03% boric acid, 20% sucrose which is a modified Brewbaker and Kwack's (1963) medium (Fig.VII). The pollen tubes attained a length of 300 μ m in 120 mts time. All the other in vitro experiments were carried out using the same medium concentrations.

4.2 EFFECT OF SELF AND CROSS PISTIL EXTRACTS ON IN VITRO POLLEN GERMINATION

Effect of self and cross pistil extracts on pollen germination and tube length were studied. In both the instances, pollen germination percentage was found to be more or less same. From the tube length, it could be observed that withania pollen attains more tube length in the media supplemented with cross pistil extract, when compared with the control over a period of 120 mts (Table 5).

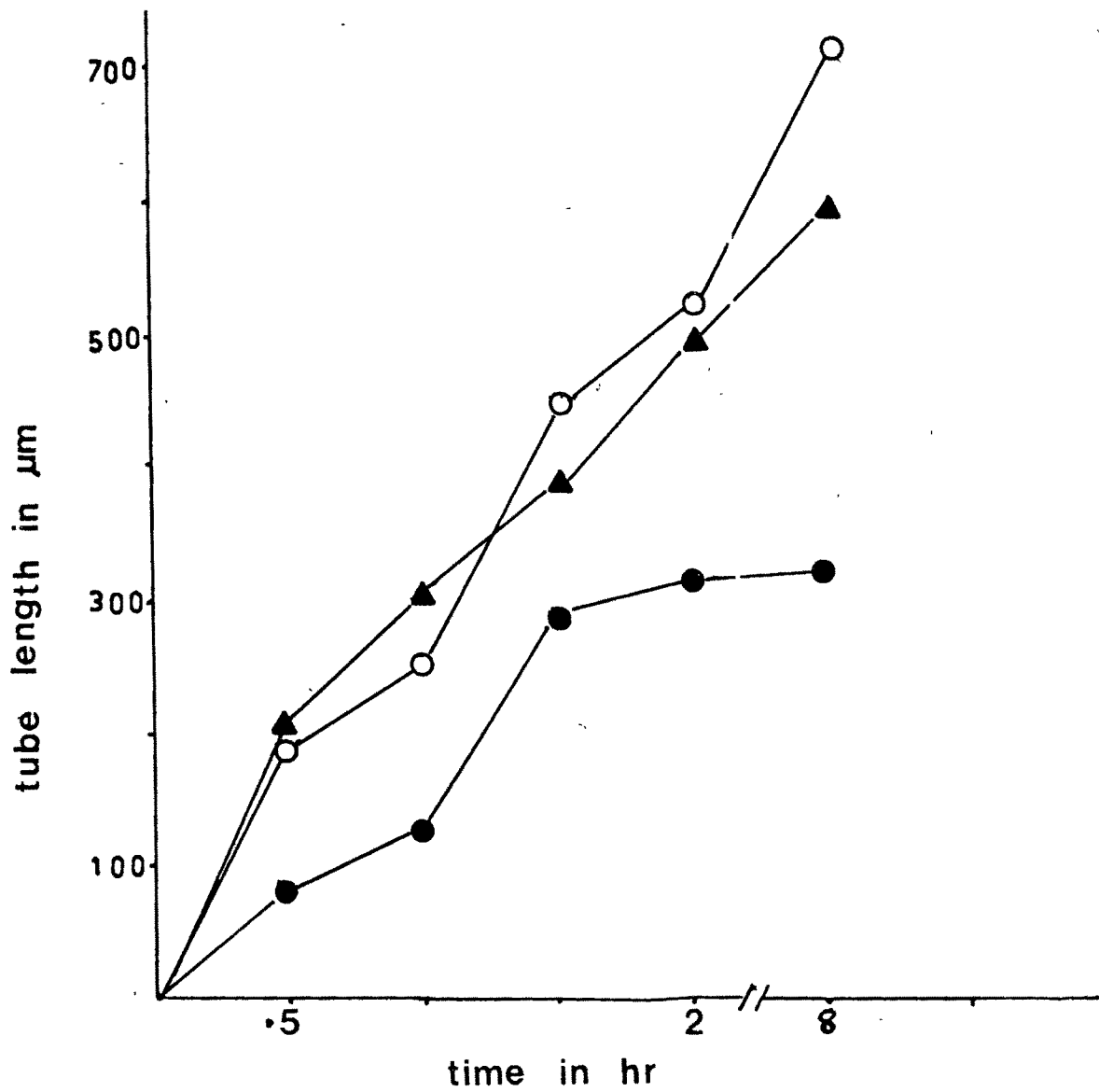


Fig. VII. Graph representing in vitro and in vivo pollen germination in W. somnifera.

In vitro (●-●); Cross pollination (○-○);

Self pollination (▲-▲).

Table 5

<u>Media</u>	<u>Tube length</u>	<u>Percentage of germination</u>
NM + self pistil extract	227	80
NM + cross pistil extract	285	80
Control	270	80

4.3 EFFECT OF SULPHUR DIOXIDE ON IN VITRO POLLEN GERMINATION

Pollen grains from freshly dehisced anthers when dusted on semi-solid nutrient medium and exposed to different concentrations of SO₂ showed a similar result as that with C. roseus. The percentage of germination and tube length showed a gradual decline as the concentration of SO₂ increased. Maximum reduction was seen at 1.5 ppm SO₂. At 0.5 ppm SO₂, the percentage of germination was reduced to 50% and the tube length reached 88 μ m in 120 mts time. At 1 ppm SO₂ the percentage germination was further lowered to 25% and the length of the tube reached 25 μ m in the same duration of time. (Fig.VIII)

4.4 EFFECT OF SO₂ ON IN VIVO POLLEN GERMINATION

Pollen germination was not seriously affected by sulphur dioxide in the in vivo condition. When compared to the control, a reduction in tube length could be observed. Maximum reduction in percentage germination and tube length was observed in the case where both pistil and the pollen were

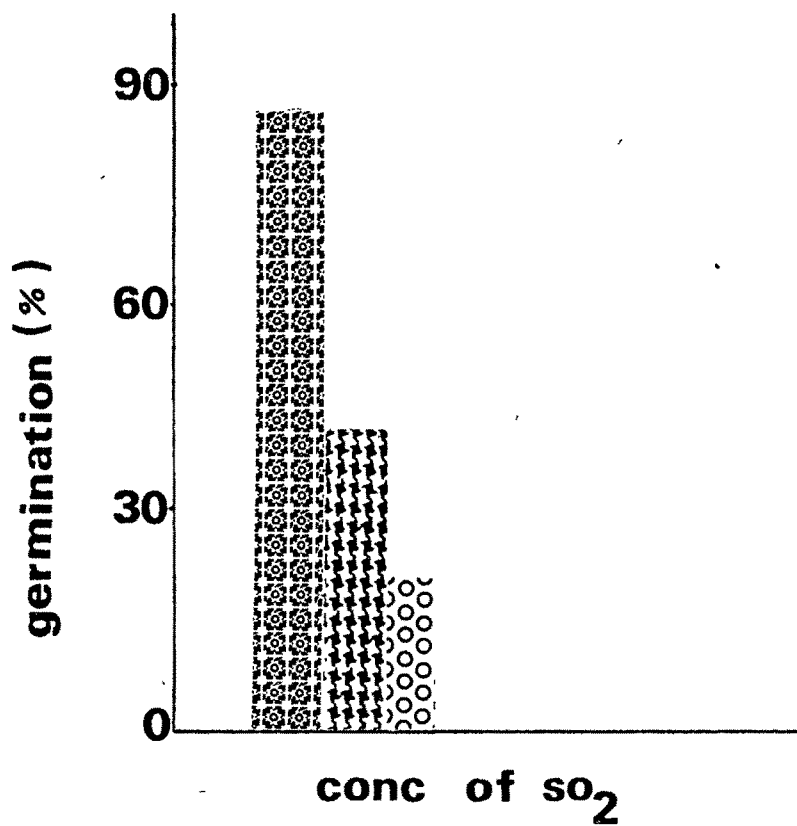


Fig. VIII. Histogram depicting the effect of SO₂ on in vitro pollen germination in W. somnifera. Control (■); 0.5 ppm (▨); 1 ppm (○).

exposed to sulphur dioxide prior to pollination. The results obtained after the various pollinations are indicated (Table 6).

4.5 EFFECT OF SPERMIDINE AND MGBG ON IN VITRO POLLEN GERMINATION AND TUBE GROWTH

Incorporation of polyamine spermidine alone or in combination with MGBG, showed that polyamine spermidine stimulates pollen germination. Incorporation of MGBG at 1.5×10^{-3} M inhibits pollen germination and tube growth. However, exogenous supply of spd (10^{-5} M) in to the nutrient medium containing 1.5×10^{-3} M MGBG after 30 mts of incubation showed a recovery in pollen germination and tube growth.

Experiments using actinomycin-D revealed a complete inhibition of pollen germination and tube growth at 10^{-9} and higher concentrations. However, incorporation of spermidine (10^{-5} M) in to the nutrient medium containing concentration (10^{-9} M, 10^{-8} M and 10^{-7} M) of Actinomycin-D showed pollen germination and tube growth. Incorporation of spermidine (10^{-5} M) in to the nutrient medium containing higher concentration of actinomycin-D (10^{-6} M, 10^{-5} M) revealed no germination at all. Results are represented in tables 7 and 8.

4.6 IN VIVO POLLEN GERMINATION

Pollination carried out using self and cross pollen indicated that W.somnifera is self incompatible. Cross

TABLE - 6Effect of SO₂ on pollen germination in vivo in W.somifera

Conc. of SO ₂ (in ppm)	Time in min.	Type of Pollination	% of germination	Tube length (μ m)
0.5	120	TS x NP	65	75
0.5	120	TP x NS	65	115
0.5	120	TP x TS	50	40
1	120	TP x NS	40	80
1	120	TS x NP	25	50
1	120	TP x TS	20	25
1.5	120	TP x NS	20	20
1.5	120	TS x NP	10	18
1.5	120	TS x TP	5	15
Control	120	NP x NS	85	265

The values are the mean of 10 observations.

TS : Treated stigma, TP : Treated pollen, NS : Normal stigma,
NP : Normal pollen.

TABLE - 7

Effect of MGBG and spermidine (SPD) on pollen germination and tube length in Withania somnifera

Treatments	Germination (%)	Tube length (μm)
Experiment 1		
Control (nutrient medium)	76 \pm 1.6	142 \pm 6.2
0.5 x 10 ⁻³ M MGBG	38 \pm 2.1	79.0 \pm 2.8
1.0 x 10 ⁻³ M MGBG	26 \pm 2.4	33 \pm 2.2
1.5 x 10 ⁻³ M MGBG	0	0
Experiment 2		
1.5 x 10 ⁻³ M MGBG	0	0
10 ⁻⁶ M SPD	15.8 \pm 3.0	62 \pm 10.9
10 ⁻⁵ M SPD	18 \pm 1.8	82 \pm 5.6
10 ⁻⁶ M SPD*	72.5 \pm 1.7	125 \pm 4.1
10 ⁻⁵ M SPD*	73.3 \pm 3.4	162 \pm 7.5
Experiment 3		
1.5 x 10 ⁻³ M MGBG	74 \pm 7.3	79.6 \pm 4.2

Expt. 1. Pollen grains germinated for 120 min in nutrient medium containing different concentrations of MGBG.

Expt. 2. Pollen grains incubated in nutrient medium containing 1.5 x 10⁻³ M MGBG for 30 min were transferred to the medium with different concentrations of SPD. Control (*), pollen grains incubated in nutrient medium for 30 min were transferred to the medium containing different concentrations of SPD.

Expt. 3. MGBG was added to the nutrient medium after 60 min of incubation.

Figures are the mean values of five experiments \pm s.e. At least 30 determinations were made for each experiment. Observations were made after 120 min of incubation.

TABLE - 8

Effect of spermidine (SPD) and actinomycin-D (Ac-D) on pollen germination and tube length in Withania somnifera

Treatments	Germination (%)	Tube length (μm)
Control (nutrient medium)	72 \pm 2.1	146 \pm 5.2
Control + 10^{-5} M SPD	75 \pm 5.2	164 \pm 7.1
Control + 10^{-5} M SPD + 10^{-9} M Ac-D	56 \pm 4.7	102 \pm 8.5
Control + 10^{-5} M SPD + 10^{-8} M Ac-D	36 \pm 1.8	53 \pm 4.4
Control + 10^{-5} M SPD + 10^{-7} M Ac-D	32 \pm 3.7	44 \pm 3.7
Control + 10^{-5} M SPD + 10^{-6} M Ac-D	0.0	0.0
Control + 10^{-5} M SPD + 10^{-5} M Ac-D	0.0	0.0
Control + 10^{-9} M Ac-D	0.0	0.0
Control + 10^{-8} M Ac-D	0.0	0.0
Control + 10^{-7} M Ac-D	0.0	0.0
Control + 10^{-6} M Ac-D	0.0	0.0
Control + 10^{-5} M Ac-D	0.0	0.0

Figures are the mean values of five experiments \pm s.e. At least 30 determinations were made for each experiment. (Observations were made after 120 min of incubation).

pollination at various stages of stigma development showed that stigma is receptive from stage II onwards (Fig.2.21 A,B). Cross pollen germinate in about 30 mts and reached the ovules in about 8 h. The pollen grains germinate on the stigma and pollen tube grew along the surface of the papillae cell towards the central depression and enters the stigma through the intercellular spaces among the transmitting tissue cells. The pollen tubes grew in tufts or individually according to the space availability and show normal callose plugging (Fig.2.21 C,D,E).

Though self pollen germinate and enter the stigmatic tissue, they get inhibited at the stylar region. Following self pollination, callose plugs are visible at the papillae cell tips as well as in the cell walls of the transmitting tissue (Fig.2.21 E,G). Bud pollination showed pollen germination in both self and cross pollination from stage II of the stigma development. However, cross pollination showed higher percentage of germination than self pollination (Fig. 1X, 2.21 G,H).

4.7 POLLEN VIABILITY AT DIFFERENT STORAGE CONDITIONS

Results of viability tests on stored pollen are plotted in a graph (Fig.X). It was observed that maximum pollen viability was retained for about 15 days in the case where pollen were stored at -4°C . At room temperature the viability was found to be lost in 10 days.

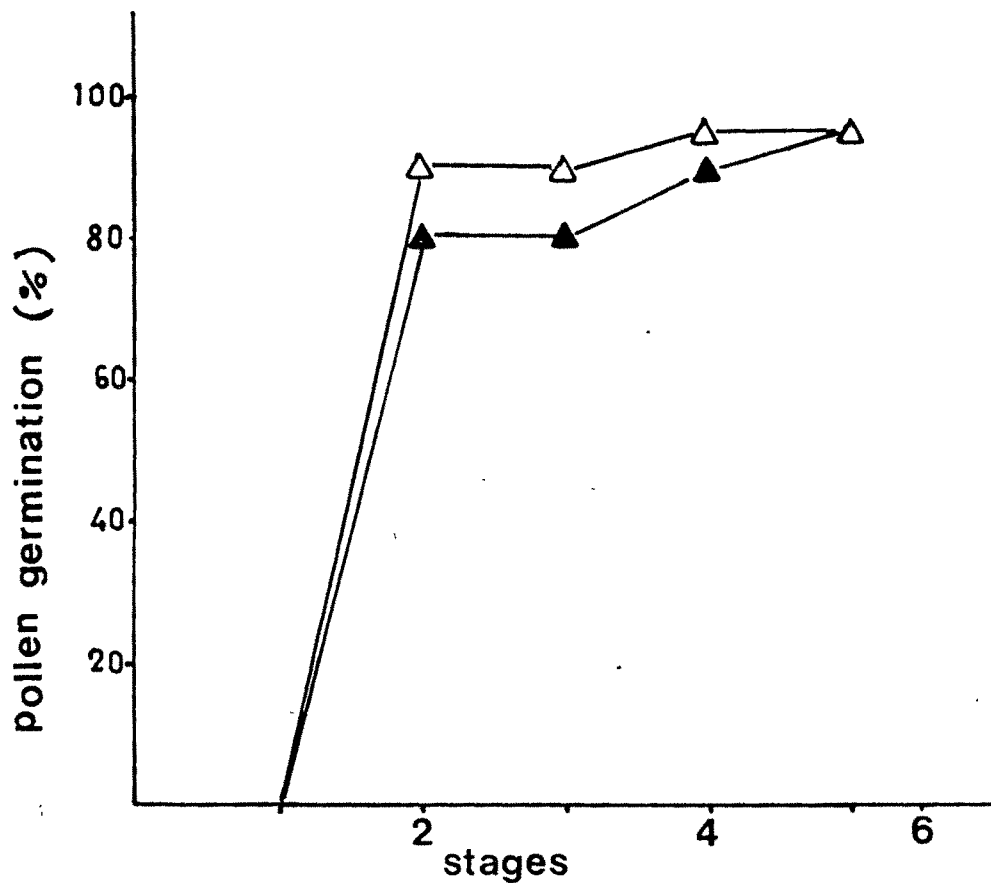


Fig. IX. Graph representing the results of bud pollination in W. somnifera.
Self pollination (▲▲); Cross pollination (△△).

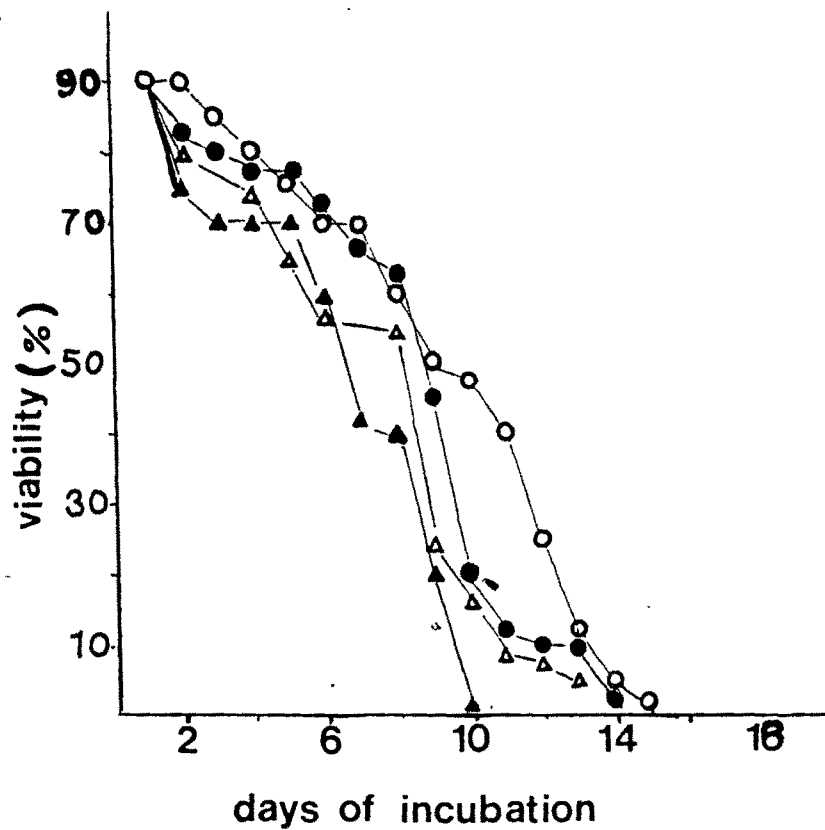


Fig. X. Graph showing percentage of viability of pollen at different storage conditions in W. somnifera.

-4°C (O-O); 4°C (●-●) dessicated condition (Δ-Δ); Room temperature (▲-▲).